A SIMPLIFIED CALIBRATION METHOD FOR THE ELECTRO-MECHANICAL SEISMIC SENSOR

By

Daniel R Burk

A THESIS

Submitted to
Michigan State University
in partial fulfillment of the requirements
for the degree of

Geological Sciences – Master of Science

2018

ABSTRACT

A SIMPLIFIED CALIBRATION METHOD FOR THE ELECTRO-MECHANICAL SEISMIC SENSOR

By

Daniel R Burk

We have developed a simplified calibration method that enables anyone to accurately calibrate an Electro-mechanical seismic station with speed, portability and low-cost. Current calibration methods generally require either expensive laboratory based equipment, or significant time and expertise. We have developed a simplified calibration method that uses an affordable industrial laser position sensor to optically track mass motion as a means of determining seismometer response. By comparing the derivative of mass displacement to seismometer coil voltage, we can determine sensitivity at any frequency within the instrument passband. The method results in the calculation of sensitivity and Poles & Zeros to within five percent. We compare the Mass Displacement Tracking (MDT) calibration method against the standard laboratory vibration table calibration, as well as the against the co-location calibration method to find that it produces equivalent results.

ACKNOWLEDGEMENTS

The author wishes to express sincere appreciation to Professors Kevin Mackey, Kaz Fujita, and Danita Brandt for their advice. I also appreciate the efforts and contributions of Dr. Hans Hartse from Los Alamos National Laboratory for his assistance. I wish to thank Ken Abrams for help with computer coding, and Albuquerque Seismological Laboratory for the use of their lab. I also want to extend my thanks and appreciation to Alexey Malovichko and his staff at United Geophysical Survey, Russian Academy of Sciences (GSRAS) in Obninsk, Russia, The Institute of Geophysical Research in Kurchatov, Kazakhstan, and the Institute of Seismology, Kyrgyzstan for their help with testing the method. I also offer a special mention for Kostia Chalyy at the Crimean Seismological Network for his technical assistance. Funding for this effort was provided by Michigan State University, the U.S. Department of Energy, and Los Alamos National Laboratory (contract # RC103610), and the U.S. Air Force Research Laboratories (contract # RC103774). Lastly, I would also like to thank my wife and kids for their patience for those times when I was away from home, working on this research.

TABLE OF CONTENTS

LIST OF TABLES

LIST OF FIGURES

INTRODUCTION

Over the past few decades, networks throughout the world have modernized seismic stations by replacing the station analog recording electronics with modern digital recording systems. In many cases, a modern digitizer is connected to an existing Electro-mechanical seismometer from the original analog station. The remaining components; i.e. the low impedance amplifiers and optical recording galvanometers are removed from service. These components however, played an integral part in determining the response and sensitivity of the seismometer channel. By removing these components, the reconfigured station channel presents an entirely different (and unknown) frequency response in terms of seismometer sensitivity and channel gain.

Without a known response curve for an instrument, it is difficult to conduct any scientific analysis beyond determining earthquake locations or seismic wave velocity studies. For example: It is not possible to accurately calculate magnitude without knowing the sensitivity of the channel. Even the routine calculation of a moment tensor solution is beyond the capability of an un-calibrated seismic station, because moment tensor solutions infer information about the earthquake energy source by modeling the earth system and instrument response and applying the model to the seismogram to approximate the source waveform. The seismogram is the output, and the earthquake is the input. They are related through the convolution of multiple linear systems:

$$u(t) = x(t) * g(t) * i(t)$$

Equation 1
(Stein and Wysession, 2003)

Where,

u(t) = the seismogram

x(t) = the energy source, such as an earthquake.

g(t) = the earth model including travel path and signal attenuation operators

i(t) = instrument response.

It is therefore important that any digital station upgrade also include an accurate re-calibration to determine the new sensitivity and frequency response characteristics of each channel.

The calibration of instrument response has frequently been ignored at upgraded stations within the seismic networks throughout the world, including parts of Russia and Asia. This is because no standardized or inexpensive field calibration methodology exists for the pairing of digital station electronics with an existing Electro-mechanical seismometer. What is needed is a general-purpose, cost-effective, and accurate calibration method that can be employed on-station. The method must be generalized enough to accommodate various combinations of seismometers and digitizer models. It must also be simple enough for engineers and technicians to apply at the local level.

The end-goal of seismometer calibration is to translate seismometer voltage output into units of ground motion. Existing calibration methods all require significant expertise, equipment, money, and time expenditures. What is needed is an inexpensive and direct way to record ground motion while simultaneously recording seismometer signal output. This thesis presents a simplified calibration method to address these needs. Although this thesis is oriented towards improving calibrations in regional and local seismic networks of the Former Soviet Union (FSU), it is also applicable to any Electro-mechanical seismometer.

CHAPTER 1: HISTORICAL CONTEXT

1.1 Historical Setting

After the break-up of the U.S.S.R., the former Soviet seismic network was split into multiple local and regional seismic networks, resulting in de-centralization of experience, expertise, and operating budgets. These networks have attempted to modernize through the use of digitizers in lieu of the historical paper record. The transition from analog to digital stations improved network capabilities in terms of earthquake locations, improved overall reliability, and streamlined access, transport, and storage of the seismic waveform records. In many of the local and regional networks of the FSU, modernization efforts did not include a well-designed calibration procedure to take into account the widely varying amplifier gain and filter configurations found throughout each network. Thus, there is doubt in the reliability of magnitude measurements, and any forward or inverse modeling based on these signals is dubious, at best.

Most seismic stations in the region use short period SKM and SM-3 mechanical seismometers that were designed for use with analog recording systems. These systems utilized a light-based galvanometer and an optical seismograph. During the late 1990s, low cost digital recording systems became widely available for the independent networks, offering lower maintenance and easier data storage capabilities. The advent of digital data enabled the networks to simplify their station operations and electronically transport their waveforms from the station to the central facility. However, as networks modernized their stations, they were left to their own devices to establish new network operating standards. The previous calibration methodologies became obsolete and regional networks were left to develop replacement calibration procedures for their many combinations of hybrid digital / Electro-mechanical seismic stations. Each newly upgraded station featured a different channel amplification, input impedance, digital resolution, and instrument response, and each parameter affected the station calibration. In networks where both funding and expertise are often

difficult to find, development of new calibration methodologies and operating standards were deferred, and then with time, likely forgotten. The problem of an unknown calibration becomes apparent by observing data trends across several different networks that operate digital instruments. In particular, shifts in earthquake K-class determinations have been noted from before and after modernization of seismic stations. For example, K-class values for earthquakes along network boundaries are often independently determined by two bordering networks. In the analog era, the network values were generally consistent to within 0.2 units. In the digital era, the difference is often larger, and sometimes exceeds a full unit (Mackey, via Pers. communication)

1.2 Development of Calibration Procedures for Digitized Seismometers

In Russia alone, 228 of 323 seismic stations deployed still use Electro-mechanical seismometers, such as the SM-3 or SKM (Malovichko, 2015) (Table 1). Additional networks outside of Russia, such as those in Central Asia, also still use these instruments. Originally designed for photo-paper recording using a galvanometer, most of these stations have now been upgraded to digital recording. Any remaining analog stations have likely been mothballed due to funding issues. A patchwork of various digital recording systems are now deployed across the networks, each with its own unique set of operating characteristics. This has led to difficulties in obtaining consistent full-station calibrations. As such, there are vast quantities of seismic data at the network not suitable for use in anything beyond basic earthquake hypocenter locations. The situation is worse because the low-impedance working coils of some older Electro-mechanical instruments are not designed to accommodate digital systems designed for high impedance sensors. The result is that the seismometer, once tuned to work with the electronics of the analog system, now operates in an unknown state of low signal output, and less-than optimal damping ratio. Each instrument configuration at each station is unique. It is therefore important to calibrate the entire system on-site, including the instrument, signal wires, and digitizer. Our intent is to develop a procedure that will

calibrate an entire system, from ground motion to digitizer output, with minimal consideration of the system details. The key to the calibration procedure we developed is the addition of a precision laser position measurement system to track mass position changes of the seismometer. We propose that mass position tracking is a suitable proxy to actual ground motion, and that calibrations may be executed in the field with as much accuracy as those generated within a laboratory. We have installed the laser measuring system on several models of Electro-mechanical seismometers currently deployed across the states of the FSU in order to develop this methodology. However, the method is general enough to be applied to any Electro-mechanical seismometer, so long as the mass is accessible for tracking movement. This would also include such seismometers as the Geotech S-13 and the IRIS AS-1. This portable calibration method can therefore improve data quality in many other networks across the world. Because of its simplicity, low cost, accuracy, and speed, the mass tracking calibration method enables researchers to quickly measure the effects of change within their Electro-mechanical seismometers.

Network	Subnet	#Stations	SM-3	SKM	SKD	Σ EM	BB + Misc.	All	EM/BB
Greater Caucuses	CMWS	39	25			25	14	39	64 %
Greater Caucuses	NORS	11	10			10	1	11	91 %
Greater Caucuses	DRS	17		7		7	10	17	41 %
Vosmochnye	KORS,OBN, MIRAS	61	19	1		20	33	53	38 %
Vosmochnye	VKMS	6	6			6	1	7	86 %
	ASRS	41	23	7	6	36	16	52	69 %
Baikal	BYKL	25	24			24	2	26	92 %
Buryatia	BURS	10	5			5	5	10	50 %
Sakhalin	SKHL	37	0	6	1	7	66	73	10 %
Yakutia	YARS	24	10	1		11	13	24	46 %
Northeast Russia	NERS	15	8			8	7	15	53 %
Kamchatka	KRSC	71	54		1	55	52	107	51 %
Krasnoyarsk	KRAR	13	12			12	1	13	92 %
Crimea (ind.)		9	9			9		9	100 %
Total:		379	205	22	8	235	221	456	

EM = Electro-mechanical seismometers such as SM-3, SKM, and SKD
BB = Broadband seismometers
Misc. = Other seismometers not suitable for the MDT calibration method

Table 1: Breakdown of seismic stations in Russian networks that could potentially utilize a simplified calibration method for Electro-mechanical seismometers (Malovichko, 2015).

CHAPTER 2: OPERATION OF THE ELECTRO-MECHANICAL SEISMOMETER

2.1 The Electro-Mechanical Seismometer

The Electro-mechanical seismometer has existed for about a hundred years. The first modern Electro-Mechanical seismometer is generally credited to Galitzin circa 1914 (Wenner, 1929). The instrument is based on the physics model of a spring-mass system with resistive damper R (Figure 1 & Figure 2). A frame containing a strong magnet is coupled to the earth. A spring suspended pendulum containing a signal coil is then hung from the frame so that the coil is placed within the static magnetic field of the magnet. A large mass is also placed onto the pendulum to provide substantial inertia in order to resist movement. The suspension of the seismometer is engineered to move freely on one axis only, with as little friction as possible. An energy-absorbing damper R couples the system back to the frame to control the system motion at the resonance frequency. The inertia of the mass prevents any movement of the pendulum within the axis unless a force is applied to the mass through the spring within the suspension. Although the mass is stationary, the frame of the seismometer is not: It moves in conjunction with the earth to which it is coupled. This has the effect of moving the magnetic field back and forth across the stationary signal coil, generating electrical signals proportional to the velocity differential between signal coil and magnet. This electrical signal represents mass velocity, relative to the frame of the seismometer. Since the frame is coupled to the earth, the seismometer signal coil outputs a voltage that is proportional to ground velocity.

The electrical signal is expressed in terms of:

$$\frac{\text{Volts}}{Meter/_{Second}}$$

In the real world, three such seismometers are generally mounted in an orthogonal orientation with positive orientations pointed to the vertical, north, and east. As seismic energy arrives at the

instrument to cause ground displacement at the instrument site, it reflects a portion of the displacement across the three orthogonally mounted components.

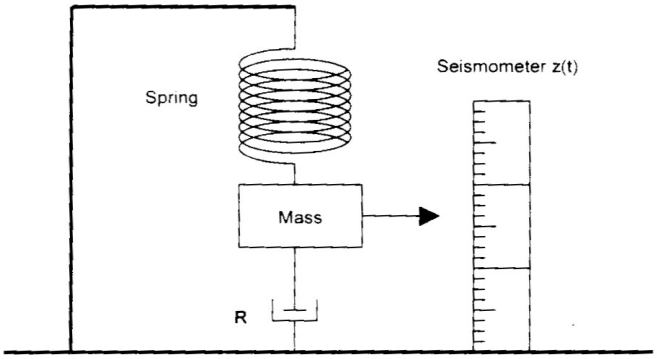

Figure 1: Cartoon of a mechanical seismometer depicted as a classical spring-mass-damper system (Havskov and Alguacil, 2004).

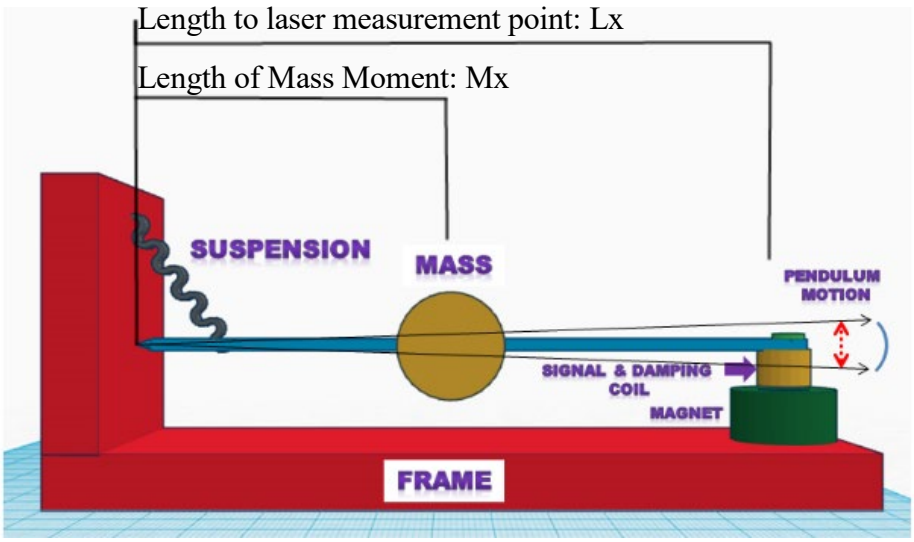

Figure 2: Cartoon diagram of a pendulum based Electro-mechanical seismometer. The seismometer oscillates about Mass Moment point Mx. The measurement of seismometer motion is made at point Lx.

2.2 Resonance Frequency ω_o (Free Period)

The Electro-Mechanical seismometer is modeled as a single spring mass system with damper (Figure 1). As such, it exhibits a resonance frequency that is a function of the spring constant k, and mass m. It is defined as:

$$\omega_o = \frac{1}{2\pi}\sqrt{k/m}$$

Equation 2
(Halliday *et al.*, 2011)

Where,

ω_o = resonance frequency

k = spring constant

m = pendulum mass

Some seismometer calibration techniques require knowledge of both the spring constant and the mass for calculating the resonance frequency. Resonance frequency is stated in units of Hertz, and is also known by its inverse function Free Period, expressed in units of seconds.

2.3 Measuring Free Period

Free Period can be measured by disconnecting as much of the electrical damping as possible, and then applying an impulse to the mass. The resulting observed oscillation occurs at approximately the resonance frequency and decays at a rate that indicates the mechanical damping ratio of the system (Figure 3). The mechanical damping within the system artificially increases the apparent free period length of the system, resulting in a reduction in resonance frequency (Figure 4). This observed free period is therefore a function of both the true free period, and the mechanical damping ratio (Equation 3). However, when the mechanical damping ratio is sufficiently small, the observed period may be assumed to represent true free period. If the mechanical damping ratio is less than 0.141, the error in the observed free period will be less than 1 % (Figure 5). According to (Havskov and Alguicil, 2004), the Electro-mechanical seismometer will exhibit a mechanical damping ratio

between 0.01 and 0.3. Thus, for most Electro-mechanical seismometers, mechanical damping accounts for 5 % or less deviation in the observed free period. In practice, the deviation is likely much less: Our observations for the mechanical seismometers that we have calibrated shows a typical mechanical damping ratio of less than 0.146 (Table 2). Therefore, the deviation of observed versus actual free period due to mechanical damping ratio is typically going to be less than 1 %.

$$\text{Observed free period } T = \frac{T_O}{\sqrt{1-h^2}}$$

Equation 3
(Scherbaum, 2001)

Where,

To = True free period

h = mechanical damping ratio

Free Period is one of the two most important characteristics of a seismometer, for it helps determine the shape and position of the frequency response curve with respect to frequency and amplitude.

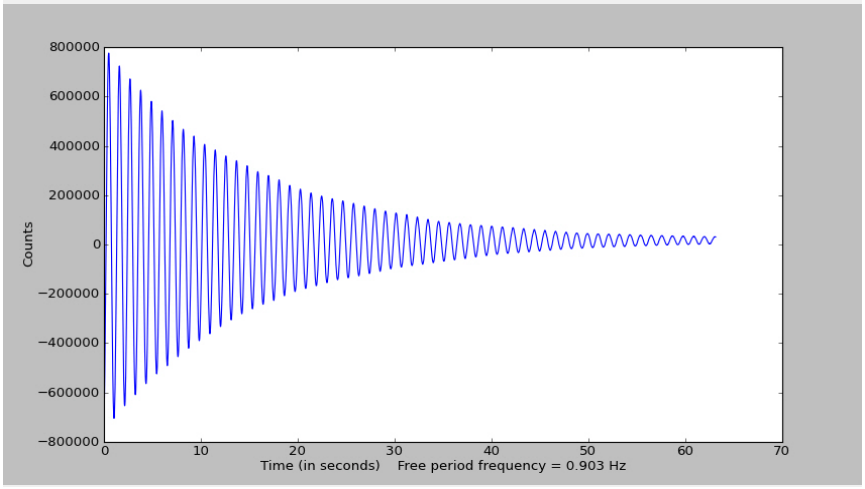

Figure 3: Decay of signal due to mechanical damping within the seismometer

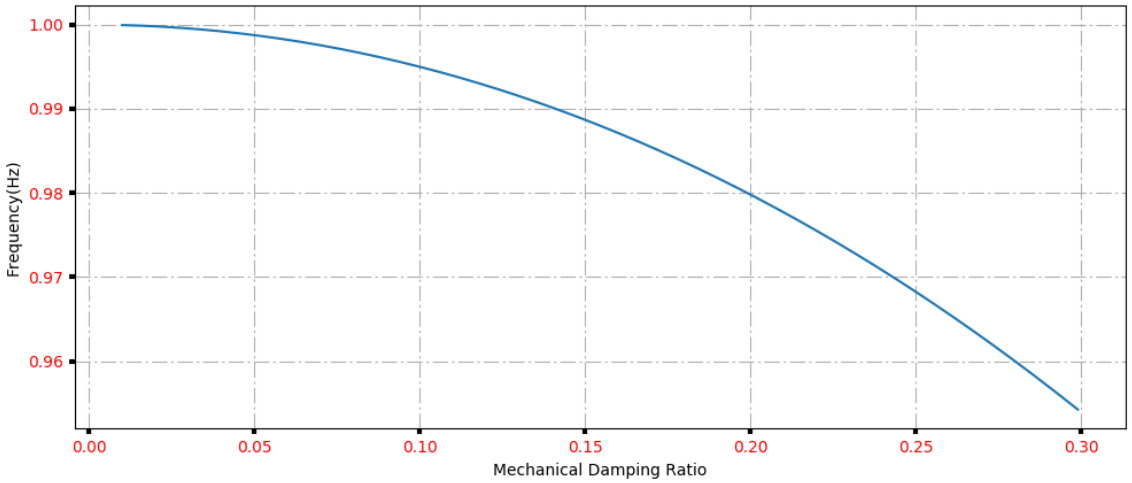

Figure 4: The reduction of observed resonance frequency as a function of increased mechanical damping from h = 0.01 - 0.3, which is the range for expected energy loss in an Electro-mechanical seismometer (Havskov and Alguacil, 2004). Plot is at 1.00 Hz true resonance frequency.

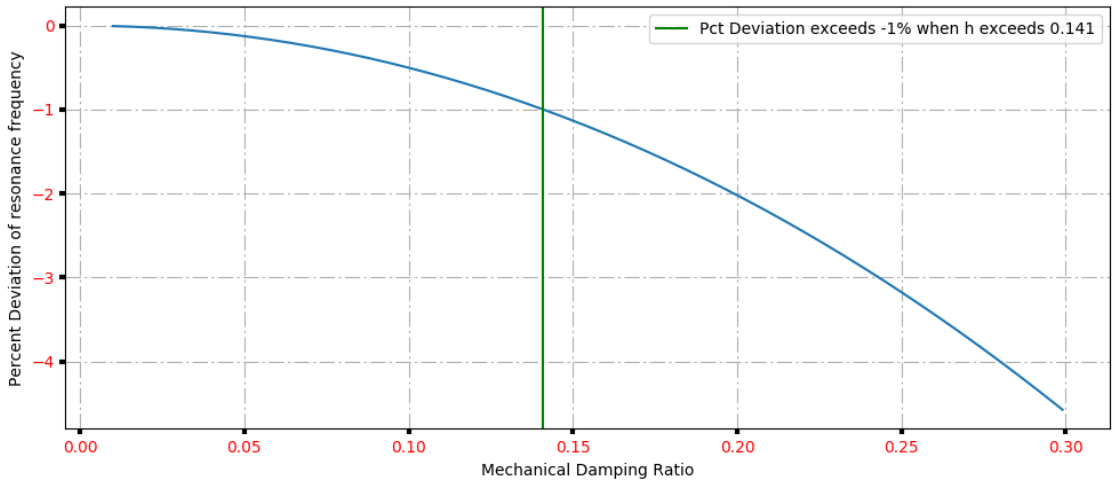

Figure 5: The percent deviation of observed vs true resonance frequency as a function of increased mechanical damping within the system. A 1 percent deviation (green line) occurs when mechanical damping ratio = 0.141

Seismometer model	Measured mechanical damping ratio
Russian SKM	0.007
Russian VEGIK	0.008
Russian SM-3	0.009
Geotech S-13	0.043
Russian S1-P	0.151

Table 2: Typical mechanical damping ratios of evaluated Electro-mechanical seismometers

2.4 Damping Ratio (h)

Damping ratio is a measure of how fast a pendulum dissipates the energy imparted into the mass to restore its static position relative to the frame and acceleration amplitude. A portion of the damping ratio within a seismometer is mechanical and is generated by air resistance and friction within the mechanics of the armature. The majority of the effective damping ratio is created by the use of some sort of tunable damper, either mechanical or electrical. Most seismometers now use an electrical damping system. A well-tuned seismometer exhibits a damping ratio less than 1, but greater than 0.6. Damping ratio is measured by imparting an impulse into the pendulum mass, then comparing two successive ‘overshoots’, where the mass moves beyond the at-rest position (Figure 6).

The size of the two overshoots relative to one another determines the damping ratio based on this equation:

$$\text{Damping Ratio } h = \frac{ln(\left|\frac{z1}{z2}\right|)}{\sqrt{n^2 * \pi^2 + ln(\left|\frac{z1}{z2}\right|)}}$$

Equation 4
(Havskov and Alguicil, 2004)

Where,

z1 = the first measured overshoot

z2 = second measured overshoot

n = number of overshoots separating the two. (Normally set to 1).

Damping Ratio is likely the most critical measurement that affects the overall calculation of instrument response. Small deviations of only a few percent will adversely affect the translation of ground motion from mass motion, especially at the resonance frequency of the instrument. A study of damping ratio measurement accuracy is carried out in chapter 5.9.6.1

Once free period and damping ratio are known, it is possible to relate the amplitude ratio and phase of ground motion to mass motion, when the system is excited at a single frequency.

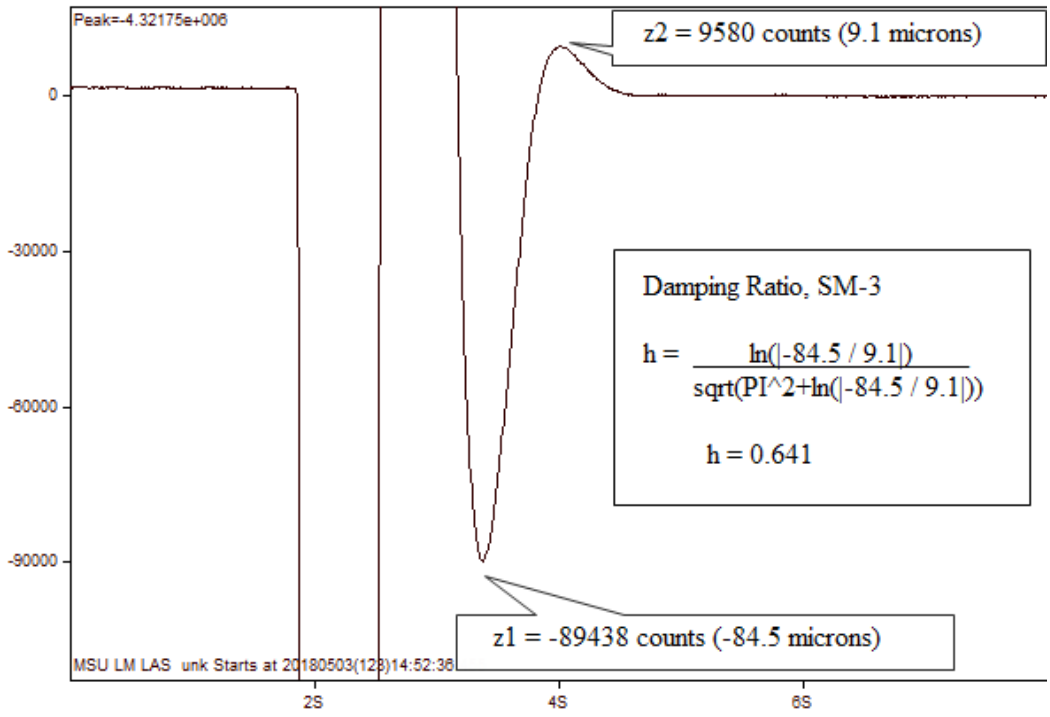

Figure 6: Sample damping ratio waveform. The rate of decay is calculated by measuring the amplitude difference between the 1st and 2nd rebound of the pendulum.

2.5 The Relationship of Pendulum Mass Motion to Ground Motion

For pendulum (Electro-mechanical) seismometers, it is possible to determine the amplitude ratio *A*, of mass motion to ground motion at frequency, ω using the following equation:

$$A = \frac{\omega^2}{\sqrt{({\omega_o}^2 - \omega^2)^2 + (4h^2{\omega_o}^2\omega^2)}}$$

Equation 5
(Havskov and Alguicil, 2004)

Where,

ω = frequency of the input ground motion signal

h = damping ratio

ω_o = resonance frequency (also known as free period)

Using this relationship, if the seismometer mass displacement is known at a specific frequency, it is only a matter of calculation to determine ground motion at that frequency. A damping ratio of 1 indicates that at resonance, the mass motion is considered critically damped. Damping ratios of greater than 1 will suppress mass motion relative to the frame. As damping ratio drops below 1, the response of the mass motion to ground motion is enhanced at the resonance frequency. At a damping ratio of ½, the mass amplitude will equal that of the frame at the resonance frequency. Damping ratios below ½ will result in a mass amplitude which exceeds that of the frame (Figure 7).

Note also, that as the input frequency decreases and approaches a dc value of near-zero, *A* approaches a ratio of zero. This is intuitively makes sense in that at very low frequencies, the pendulum of the seismometer has enough time to "catch up" to equilibrium while the frame moves with earth motion. It therefore experiences very little displacement relative to the seismometer frame. As frequency increases, and $\omega >> \omega_o$, the mass to frame amplitude converges on the ground motion amplitude, yielding $A \approx 1$. The mass stays stationary while the frame moves back and forth around it.

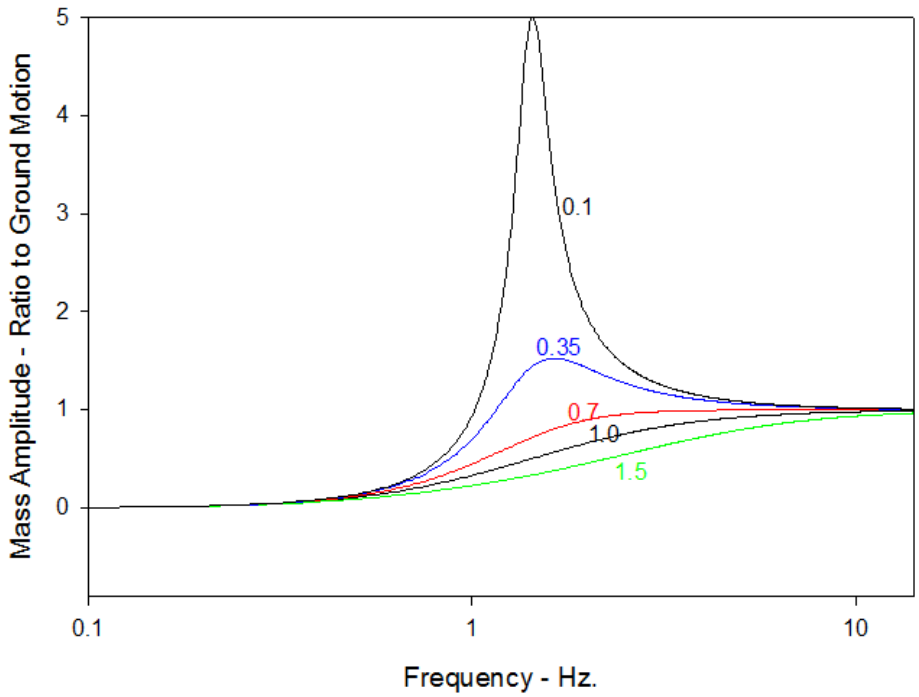

Figure 7: How pendulum amplitude changes with damping ratio. As damping ratio gets smaller, the relative amplitude change at resonance frequency gets larger.

2.6 The Relationship of Pendulum Phase to Ground Motion

If the frame is excited at low input frequencies, the mass motion lags behind the frame motion by only a small number of degrees, and mass displacement relative to the frame is low. At resonance, mass motion lags frame motion by $-\frac{\pi}{2}$ radians, causing it to oscillate at its greatest displacement. As input frequency increases even further, mass motion continues to lag frame motion until it reaches a maximum phase shift of -2π. This phase relationship is a function of resonance frequency, input frequency, and also damping ratio. Damping ratio plays an especially important part in determining the rate of phase change when close to the resonance frequency of the instrument (Figure 8).

Phase response Φ, as a function of ground motion frequency ω and is calculated based on the formula:

$$\Phi(\omega) = \text{atan}\left(\frac{2h\omega\omega_o}{{\omega_o}^2 - \omega}\right)$$

Equation 6
(Scherbaum, 2001)

Where,

ω_o is the resonance frequency

h is damping ratio.

Once we know the characteristics of the seismometer, namely: resonance frequency, damping ratio, and ground motion to mass motion ratio A, it is possible to use mass motion as a proxy measurement for ground motion at all frequencies within the measurement range of the instrument.

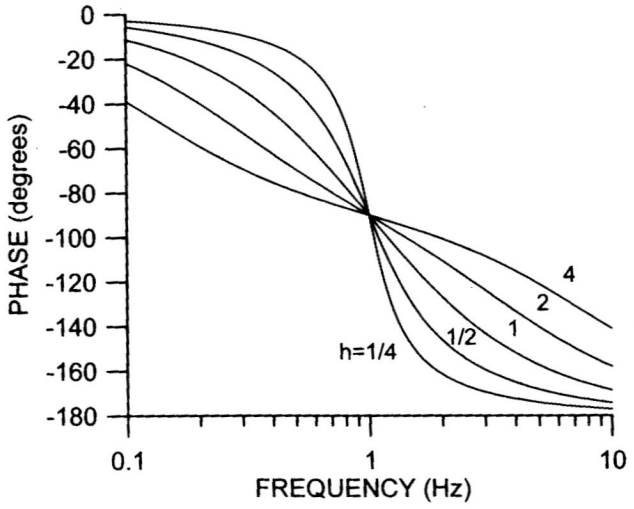

Figure 8: Frequency versus phase with a 1Hz resonance frequency and various damping ratios (Havskov and Alguacil, 2004).

2.7 Mathematical Relationship of Displacement, Velocity, Acceleration

The science of motion is based on four principal observations:

Starting position *x*. This is the object's initial condition in space and time.

Displacement *dx*: This is how much an object's position has changed.

Velocity *dx/dt* : This is how fast an object's position is changing.

Acceleration d^2x/dt : This is how fast the velocity is changing.

If a time-varying signal representing velocity or acceleration is observed, it is possible to calculate the resulting displacement based on the integral, or 2nd integral of the signal respectively.

If a time domain signal representing motion is constrained to a single, sinusoidal frequency of stationary amplitude, the relationship between acceleration, velocity, and displacement simplifies to a function of the angular frequency ω.

If the input signal is purely sinusoidal in nature, then at any given frequency *f* (in Hz):

$$\text{Peak displacement } X = \frac{-V}{2\pi f} \qquad \text{Equation 7}$$

Where,

X = peak amplitude of displacement of the seismometer mass in meters

V = peak velocity of the seismometer mass in meters/second

And,

Velocity V can also be expressed as Aω

Where,

A = amplitude of the displacement signal in meters,

ω = oscillation frequency in terms of 2π radians/second.

Thus, displacement X is expressed as:

$$X = \int A\omega = -V/2\pi f, \text{ (using equation 7)}$$

The negative value in the result means that displacement lags velocity.

When the input signal is a periodic sine function, displacement and velocity are related by the term $2\pi f$ and vary only by phase. This relationship greatly simplifies the translations when comparing separate measured signals of velocity and displacement within a seismometer and enables the comparison of mass displacement to the mass velocity. This is why many of the basic calibration methods, when calculating within the time domain, separate the calibration into a series of stationary, periodic sinusoidal signals.

2.8 The Electromagnetic Damping Circuit

An important development for the Electro-mechanical seismometer was the introduction of the electromagnetic damping circuit by Wenner in 1925 (Wenner, 1929). By replacing the oil-filled mechanical damper of previous seismometers, the new circuit enabled stations to fine-tune the seismometer's frequency response with a simple electrical resistor. This resistor is placed in one of two places: Either across the output terminals of the signal coil, or as a shunt resistor on a separate damping coil that is co-wound along with the signal coil (Figure 9). One important note is that the damping circuit is both a function of the damping resistor, and the input impedance of the recording device. In analog systems, the recording device was typically a miniaturized, low impedance electrical motor within an optical galvanometer. In digital systems, it is the input impedance of the digitizer, which ranges widely from 20 Kohm to 1 Megaohm. Thus, the damping circuit performance (and consequently, the seismometer frequency response characteristic) is highly dependent upon the input impedance of the recording system, whether analog or digital in nature.

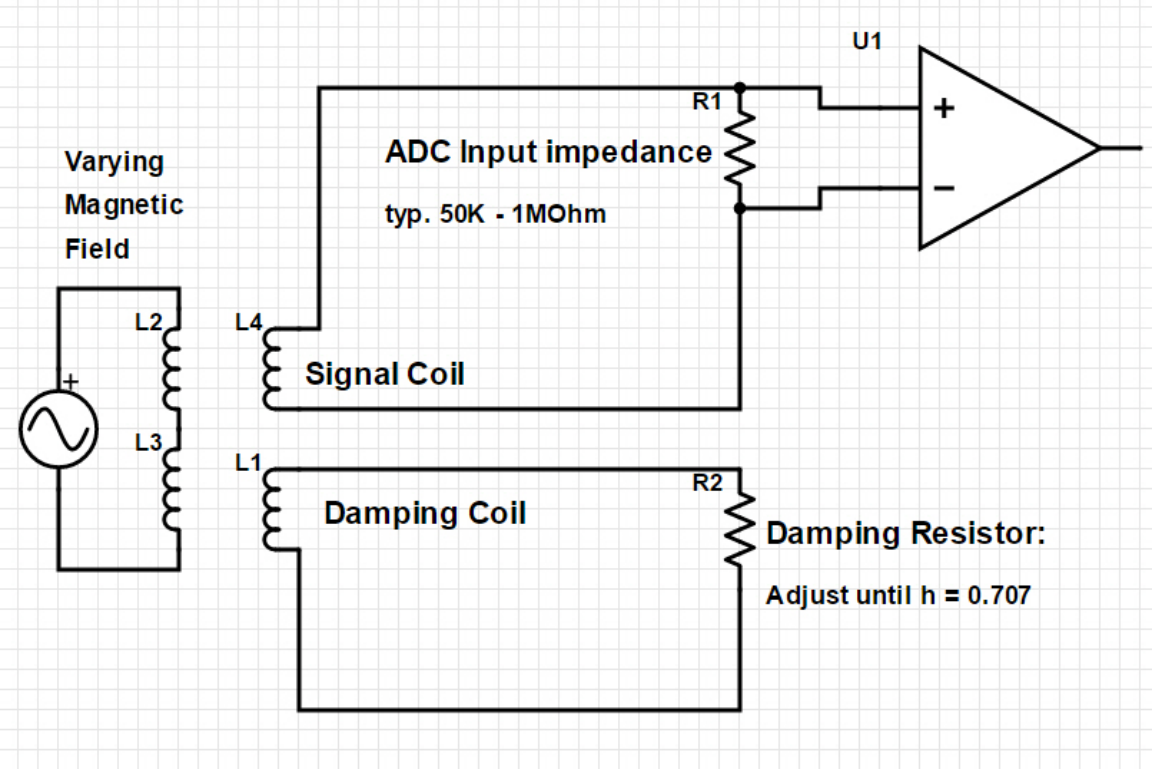

Figure 9: Equivalent circuit for the Electro-mechanical seismometer with electronic damping.

CHAPTER 3: REVIEW OF EXISTING CALIBRATION METHODS

3.1 Vibration Table Within the Laboratory

Likely the best way to calibrate the Electro-mechanical seismometer is by using a vibration table within a laboratory. The vibration table is placed upon a large concrete pier to isolate extraneous movement, as well as to ensure a good, stable thermal environment. The table is designed to isolate a single axis, so that all induced motion is within the measurement plane of the test seismometer. The table is outfitted with a precision Linear Variable Displacement Transducer (LVDT) that records the motion of the table. In this sense, the table motion is the equivalent of ground motion. A signal generator and power amplifier supply the table with a single frequency, stationary amplitude signal necessary for generation of periodic motion. The LVDT then directly measures the resulting ground motion imparted into the frame of the reference seismometer. By comparing the voltage output of the seismometer to table displacement at various frequencies, a precision measurement of the instrument response can be obtained.

A vibration table is an accurate method for calibrating a seismometer, but there are some disadvantages to this method in terms of cost and logistics. A vibration table capable of replicating low-frequency and low displacement ground motion is difficult and expensive to design and fabricate. Understandably, there are very few facilities with such tables. Two such facilities are Albuquerque Seismological Laboratories (ASL) in Albuquerque, New Mexico, USA (Figure 10), and the United Geophysical Survey, Russian Academy of Sciences (GSRAS) in Obninsk, Russia. Another disadvantage to the vibration table is that it is difficult to calibrate the ‘whole system’. Though a network might be able to ship the seismometer to the laboratory, an Electro-mechanical seismometer is only part of the system that determines frequency response. The signal wires and the input impedance of the digitizer also play a key component to the frequency response of the channel. Since the input impedance of digitizer models varies widely, it is very difficult to obtain a precision

calibration using this method. For the input impedance of the digitizer plays a critical role in determining the damping ratio of the seismometer. We have observed official calibrations go awry when the sensor was re-deployed into the field because of the various digitizer input impedances that were unaccounted for during the time of laboratory calibration. These variances result in an instrument that may be significantly over-damped in the field, thus adversely changing the entire frequency response of the channel (See section 2.7).

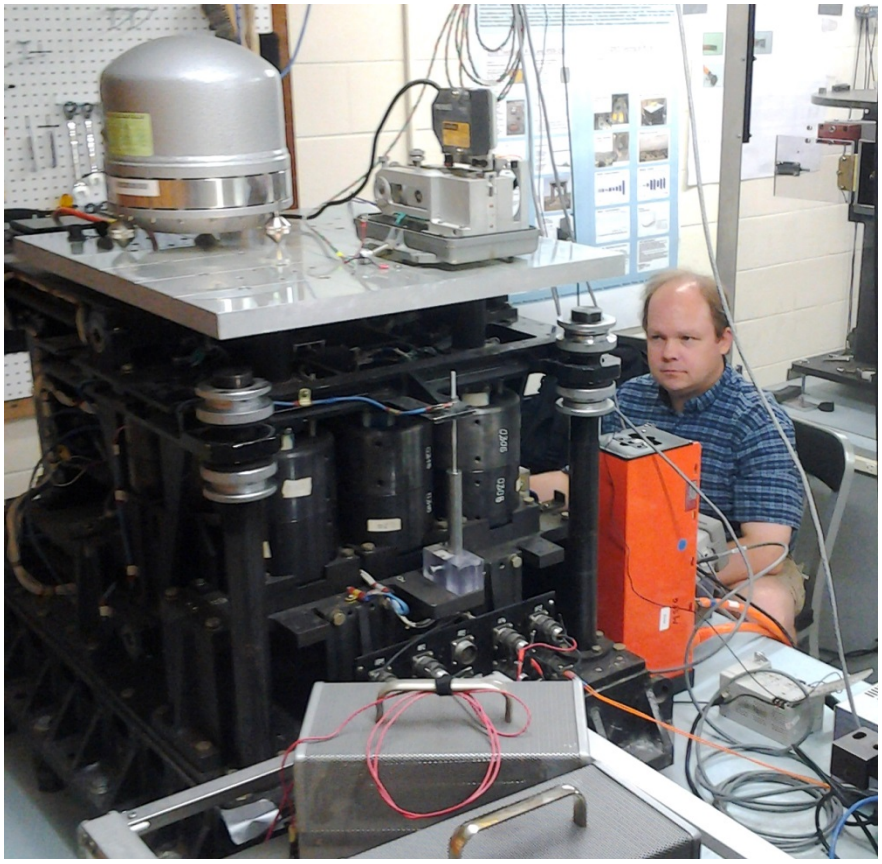

Figure 10: Vibration table at Albuquerque Seismological Laboratory (ASL), Albuquerque, NM

3.2 Step Impulse

Step impulse calibration has existed in various forms since the introduction of the seismometer. The technique has changed over time to accommodate the analog galvanometer, and consists of a perturbation of the seismic mass, either physically, or electrically via a calibration coil. Physical perturbations of the seismic mass are difficult to execute with precision. The use of a calibration coil is significantly better, but requires careful measurement of applied current, and knowledge of the calibration coil motor constant. Unfortunately, a significant number of the Electro-mechanical seismometers are not equipped with calibration coils. The step impulse technique was refined by Rodgers (1995) by applying a step impulse to the signal coil itself. This technique requires knowledge of the precise weight of the mass within the seismometer. This information is not always available, as is often the case for many of the older instruments still employed in the field. Rodger's technique has promise, but also requires the seismometer to be coupled to a recording system with high input impedance such that it does not influence the seismometer damping circuit. Since there are such a wide variety of input impedances in the many models of digitizers used in the field, the impedance requirement of any given seismic station cannot be guaranteed. Because of the impedance requirement and the generally unknown state of the seismometer mass, the step impulse technique cannot be applied universally across seismic networks.

3.3 White Noise Injection

White noise injection requires the use of a precision arbitrary waveform capable signal generator, a good current amplifier, a calibration coil, and signal analysis software to analyze the waveforms in the frequency domain. The specialized equipment, software and the expertise to employ this method make it difficult to apply with consistency across seismic networks.

3.4 Co-location

Co-location involves the placement of a reference seismometer directly adjacent to the instrument under test for time periods of several hours to several days. The temporarily deployed seismometer will then measure the same signals as the test seismometer. The signals are then both converted to units of equivalent ground motion and analyzed within the frequency domain. By comparing the difference between the two signals, co-location can generate a correction factor that can then be applied to the existing response curve of the test instrument. This results in a response curve for the test unit that matches the response of the reference seismometer. The method is robust but requires an expensive reference seismometer that can be deployed into the field for an extended amount of time. Therefore, there are logistical hurdles to be overcome when using this method, such as equipment cost, maintenance, and transportation of both the reference instrument and the network staff. It also requires trust on the part of the station manager that the ‘reference’ seismometer has itself, been accurately calibrated against another standard.

CHAPTER 4: CALIBRATION THROUGH MASS DISPLACEMENT TRACKING

The method of calibration via mass displacement tracking is similar to the vibration table calibration method, which creates frequency-controlled ground motion by moving the whole seismometer at a specific frequency and then measuring the signal output. For, if seismometer voltage signal output is compared to a known ground motion, the seismometer sensitivity is a matter of basic math. Yet, it is difficult to generate a precise ground motion without a laboratory-installed vibration table. It is not as difficult, however, to generate mass motion in the field: All it takes is a small excitation coil, magnet, and a sine wave signal generator.

Equation 5 states that for any Electro-mechanical seismometer, ground motion may be calculated based on the measurement of damping ratio, free period, and the pendulum mass motion. Therefore, if damping ratio and free period are known, the response of the system as a function of voltage output versus ground motion is measurable if one can accurately measure the mass motion. If mass motion does truly describe ground motion as asserted in equation 5, then field measurement of mass displacement should be a suitable proxy for the large and expensive laboratory-based vibration table. Thus, mass displacement tracking should likewise provide a calibration method with similar precision as that of the vibration table. Part of the elegance of this calibration method is that it takes the calibration back to base-units of measurement: Time, displacement, and voltage, that are independently verifiable to great accuracy.

4.1 Measuring Mass Displacement via Laser Position Sensor

The precise measurement of the mass displacement in a field environment is difficult: The measurement itself must not influence the motion of the mass or it will render the calibration invalid. This limits the application to non-contact measurement techniques. However, any technique must be both accurate and linear over a huge dynamic measurement range. Over periods of several seconds to frequencies of several Hertz, the peak displacement of the seismometer can vary from several microns to several millimeters. Thus, the measurement technique must be capable of measuring with high resolution over long distances. The most suitable measurement system is optical tracking via laser. Modern laser position sensors are now capable of accuracy to less than one micron. Historically, displacement transducers that meet these specifications were exceedingly expensive and rivalled the price of a new seismometer. However, surplus industrial laser position sensors have recently come to market that are both economical and capable of providing measurements sufficient for tracking the mass of the instrument.

4.1.1 Laser Position Sensor

The heart of the mass displacement calibration method is the Keyence laser position sensor (Figure 11). These surplus industrial units are inexpensive, readily available, and capable of resolving mass movement from 10 millimeters to 1 micron over a frequency range of dc to about 15 Hz, which covers the operating conditions of almost every Electro-mechanical seismometer still in use today. The single qualifying condition is that the mass of the seismometer must be accessible for optical tracking by the laser position sensor. Fortunately, most weak-motion Electro-mechanical seismometers, (with exception to geophone-based instruments) can be adapted for the optical tracking of the mass.

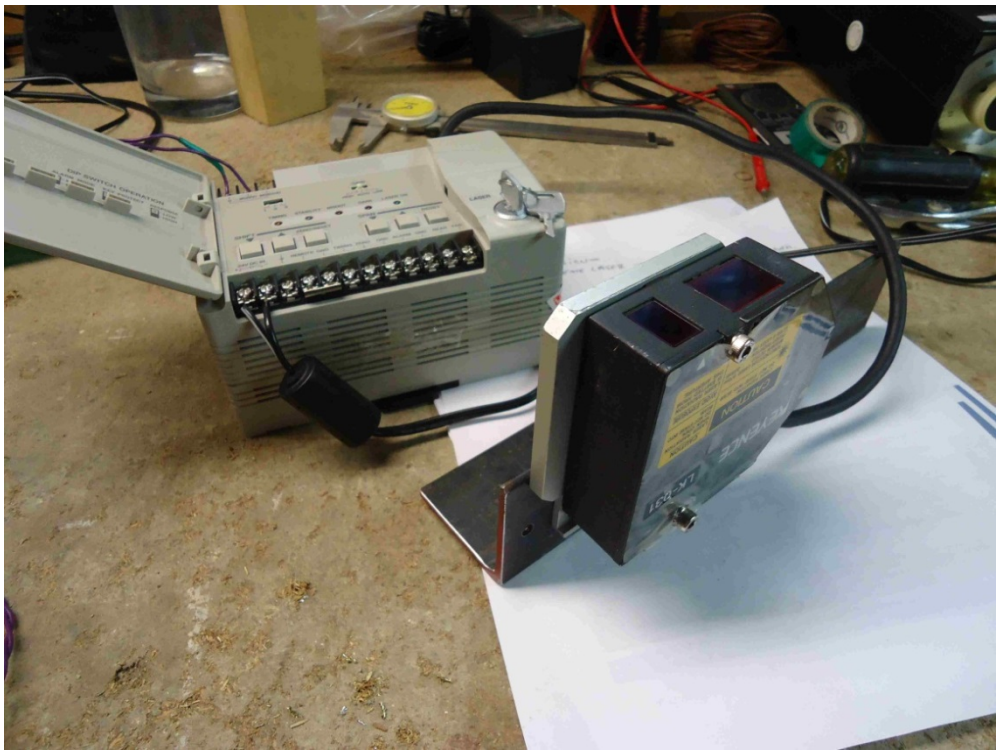

Figure 11: Keyence LK-31 laser and LK-2001 control box for precision measurements.

4.2 Creating Equivalent Ground Motion via Excitation Coil

It is difficult to precisely excite a seismometer frame to replicate ground motion without the use of a laboratory-grade seismic shake table. This is especially true when attempting to calibrate a seismometer when it is still in the seismic vault. However, it is easy to excite the seismometer mass, rather than the frame, by applying a time-varying current into a small, frame mounted excitation coil that pushes against a miniature, pendulum mounted rare earth magnet (Figure 12).

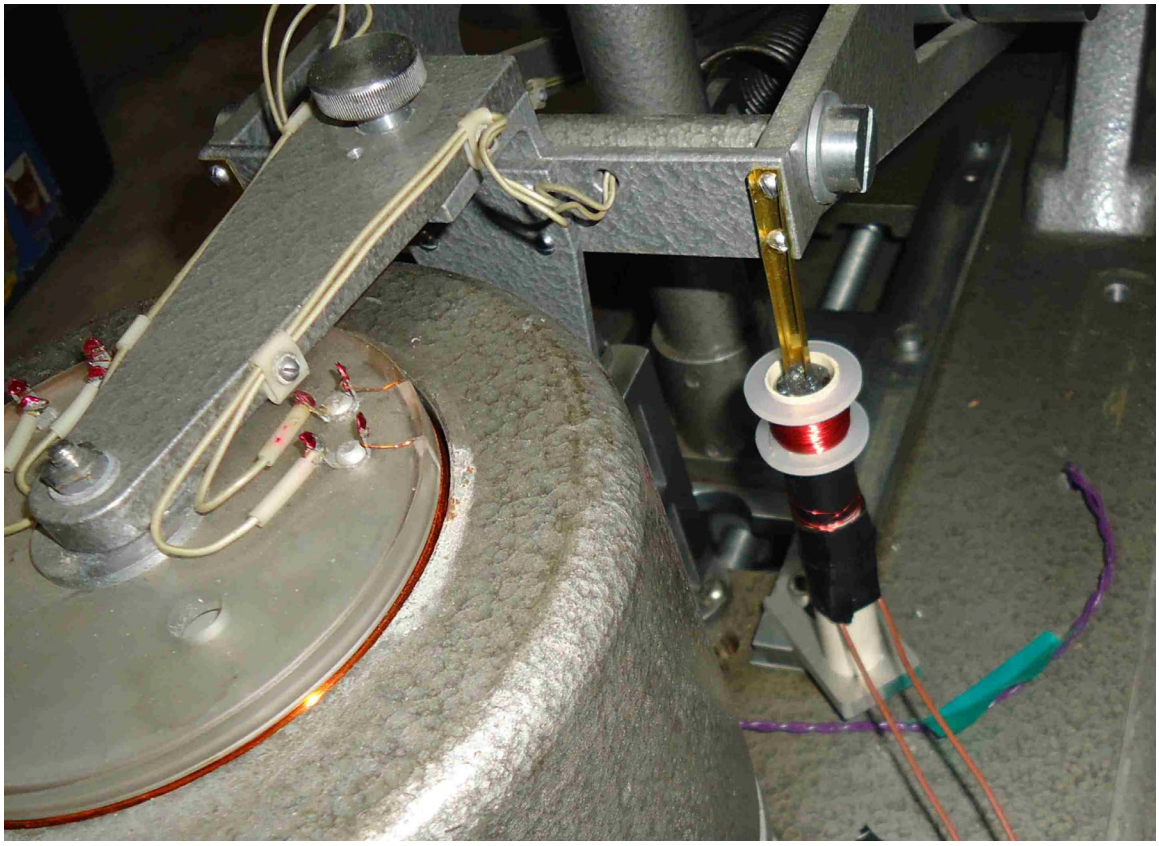

Figure 12: Excitation coil mounted on the base of a Russian SKM seismometer. The armature-mounted brass fixture contains a small neodymium magnet that enables us to apply a sinusoidal electromotive force to the pendulum with a signal generator.

The excitation coil is mounted such that it is physically distant from the seismometer signal coil to prevent inductive cross-coupling between the two coils. The current applied to the excitation coil will exert an arbitrary force against the excitation magnet and result in an arbitrary amount of mass displacement. It is no longer necessary to precisely measure the applied current or even the motor constant of a true calibration coil, because we now directly measure both the seismometer mass displacement and signal coil voltage output representing the corresponding mass velocity (Figure 13). Therefore, the force applied to the system is allowed to be arbitrary, so long as it creates sufficient mass motion for adequate displacement measurement by the laser position sensor. The

induced arbitrary mass motion by the excitation coil thus serves as a proxy for the ground motion signal of the otherwise expensive (and impossible to transport) laboratory vibration table.

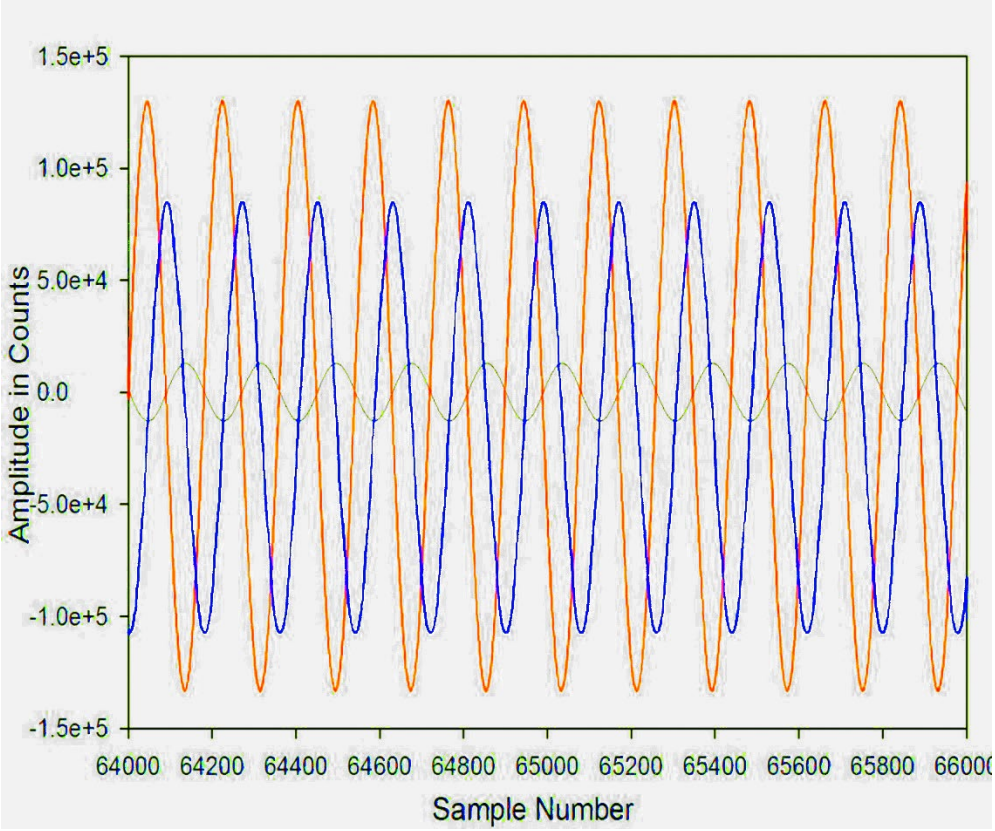

Figure 13: Measurement of excitation coil current (red), mass displacement (blue) and seismometer signal coil voltage output (grey) Because mass displacement energy and signal coil voltage representing velocity are mathematically related, excitation coil current measurement is no longer necessary.

4.3 Calibration Methodology

It has been shown that ground displacement may be derived from mass displacement if the resonance frequency and damping ratio of the pendulum are known (section 2.5). It has also been shown that ground velocity is the mathematical derivative of ground displacement (section 2.7). It has also been shown that the Electro-mechanical seismometer signal coil yields a voltage that is proportional to ground velocity (section 2.1). Therefore, the sensitivity of the signal coil may be derived by dividing the signal coil voltage by the derivative of equivalent ground motion as measured by the laser position sensor. Because the signal coil sensitivity is not linear over the bandwidth of the instrument, it is necessary to make measurements at multiple frequencies (break-points) across the passband of the seismometer. The goal is to relate the sensitivity measurement as a function of ground motion velocity at frequency ω:

$$\text{Units of Velocity } S(\omega) \text{ at frequency } \omega = \frac{Volts}{Meter/second}$$

When the measurements are assembled into a curve, the resulting frequency response curve describes the voltage sensitivity response of the seismometer as a function of frequency (Figure 14).

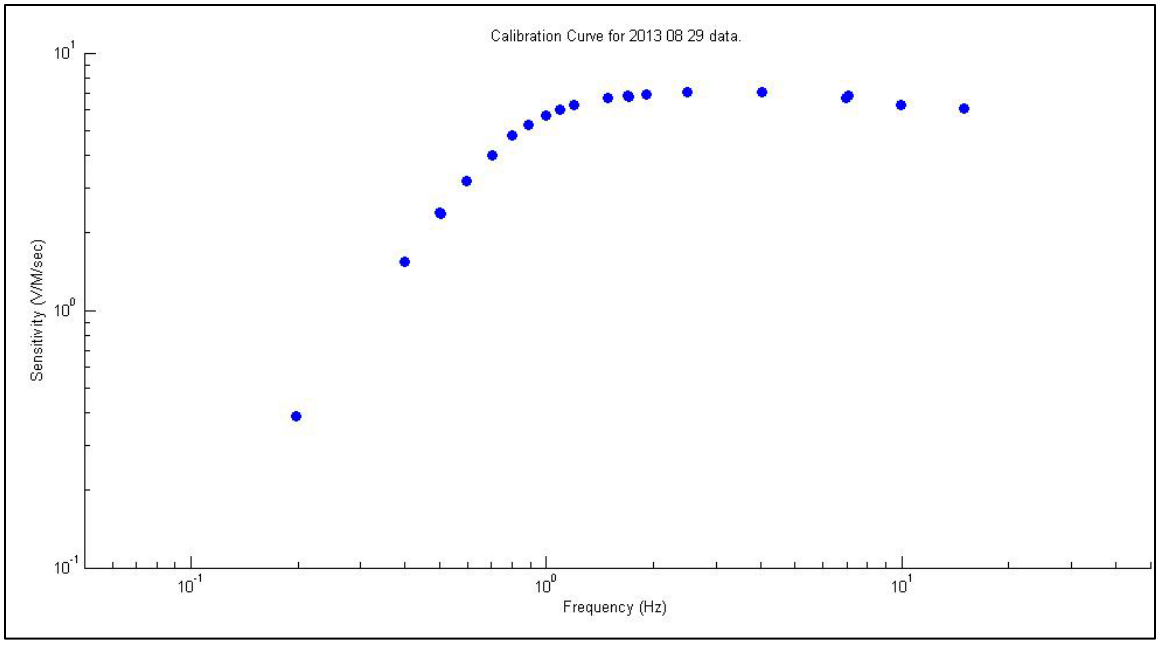

Figure 14: Seismometer voltage sensitivity curve at 18 different frequencies.

4.4 Ratio of Target Displacement to Mass Displacement : LCAL Constant

The measurement of equivalent ground motion is always specified at a point along the pendulum called the center of oscillation. (Figure 2). The Mass moment, which is the length from pivot point to the center of oscillation, is not easily derived and requires disassembly of the seismometer. Some seismometers require a laser target that cannot be directly centered at the center of oscillation, and may reside some distance away, somewhere else along the length of the pendulum. This means that the measured displacement by the laser may be larger or smaller than the actual mass displacement: A laser calibration correction factor (LCAL) is therefore required. The mass displacement is derived from the laser displacement through the following relationships:

$$LCAL = \frac{mx}{lx}$$

Equation 8

Where,

mx = distance from fulcrum to the center of pendulum mass (mass moment),

lx = distance from fulcrum to the center of the laser target.

And,

$$\Delta My = \Delta Ly * LCAL$$

Equation 9

Where,

ΔMy represents mass displacement,

ΔLy is the measured laser target displacement.

Assuming the measurement point is standardized on a given model of seismometer, LCAL varies little between seismometers, and the small variances that might arise from manufacturing tolerances should not significantly affect the accuracy of the calibration. Therefore, LCAL is a quantity that can be measured within the lab and published. (Table 3).

Some seismometers such as the S1-P and the Geotech S-13, have the mass co-linear with the measurement axis. For the Vegik, it is easy to mount the laser measurement point at the center of mass. In these cases, $lx = mx$, and the correction factor converges on 1.0

Seismometer Model	LCAL Constant
SKM Vertical	0.550*
SKM Horizontal	0.340*
SM-3 (vertical or horizontal)	0.579**
S1-P	1.00
VEGIK	1.00
Geotech S-13	1.00

Table 3: Laser calibration correction factors for various seismometer models.

(* SKM LCAL measured at institute seismology, Bishkek, Kyrgyzstan.)

(**SM-3 LCAL measured at GSRAS, Obninsk, Russia.)

CHAPTER 5: DEVELOPING THE MASS DISPLACEMENT TRACKING CALIBRATION METHOD

Initial tests involved the use of both the Soviet SKM-3 and the Soviet-era SM-3 vertical seismometers. We developed bracket designs for both seismometers that can be hand-fabricated by technicians in the field with basic shop tools. Each seismometer was then fitted with a Keyence LK-31 laser position sensor, a small magnet, and a hand-wound excitation coil. The excitation coil is connected to a sine wave signal generator to simulate ground motion by moving the seismometer pendulum. Forced ground motion at the seismometer frame is unnecessary, because equation 5 demonstrates that we can substitute pendulum (mass) motion for ground motion, so long as the damping ratio and oscillation frequency (Free Period) of the seismometer are determined. Therefore, it is possible to calculate ground motion by measuring mass motion via the laser position sensor.

5.1 Step 1: Know Your Instrumentation Sensitivities

The calibration system involves several key components that must first themselves be calibrated, or at least measured:

5.1.1 Digitizer Gain for Signal Coil and Laser Position Sensor Channels

Digitizers, (also known as Analog to Digital Converters (ADC)) are counters that divide an input signal by a reference voltage to arrive at a ratio representing the percentage between zero and full-scale. They then convert the resulting ratio into a digital value known as counts. The number of counting bits featured by the digitizer determines the gain of the measurement, and the gain is reported in terms of counts per volt. It can also be reported in terms of microvolts per count. As an example, if a 24-bit digitizer can measure +/- 8 volts (16 volts total range), it's theoretical gain is 16V/(2^24) counts, or, 0.954 microvolts per count. Although this figure is generally close, it is not sufficient to use this value within a calibration without first verifying the figure. Our investigations have shown that the gain of some digitizers may deviate by greater than one percent. Our worst

observed deviation in an ADC channel gain was -1.3 %. Because subsequent measurements are based on the accuracy of these digitizer channels, measurement errors due to a deviation of the ADC gain will propagate throughout the calibration chain. It is therefore important to first calibrate the digitizer by applying two precision dc voltages to each input channel, then measure the output in counts to verify the channel. A simple +/-1.000 Volt, dc reference signal will generally result in a count measurement of over 1:1,000,000 for most 24-bit digitizers. This gain measurement is then recorded and used during subsequent calculations to convert the digitizer measurements from units of counts, into units of volts. It is assumed that any digitizer non-linearity is significantly less than 0.1 % and is therefore not accounted for.

5.1.2 Laser Position Sensor Sensitivity

Like the digitizer, the laser position sensor is a digital device that converts distance in microns into units of volts. Our method relies on the supply of second-hand laser position sensors that have been replaced in industry applications. As such, the gain of the system is frequently unknown. Additionally, the gain of the laser position sensor is at the controller. Therefore, it is important to verify gain and linearity. The gain and linearity of the laser position sensor is verified by installing the laser onto a fixture in which a reflector is moved from a starting position to an ending position. The change in voltage, divided by the change in distance will verify the gain. By making multiple measurement points along the axis, linearity of the measurement is likewise verified. We have fabricated a fixture that uses a digital caliper to calibrate each laser position sensor (Figure 15). The sensors themselves are received from the seller with laser heads that frequently no longer match with the controller. Thus, gains may vary by as much as five percent from the nominal value of 1.000V / mm (which is also 1.000 uV/micron). However, upon calibration, we find that the LK-31 gains are linear across their 1 cm range. We also tested the laser system at cold temperatures (down to -26^{o} C) to ascertain field operation in winter conditions (Figure 16). There is no measurable change in

system gain or linearity between warm and cold environments. Any measurement error of gain deviation will result in a direct measurement error in the calibration of sensitivity. By manually calibrating the laser over its full range, the gain can be verified to well within 0.1 %

Figure 15: Laser position sensor calibration fixture used to verify sensitivity and linearity.

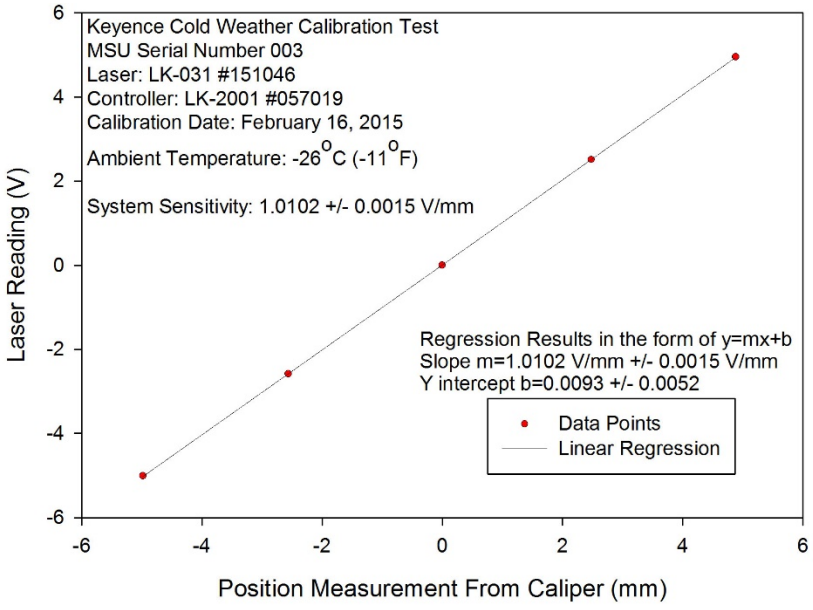

Figure 16: Calibration of the Keyence LK-31 laser position sensor in a cold (-26 deg C) environment

5.2 Step 2: Measuring Free Period

Free Period is the inverse of the resonance frequency and is described in units of seconds. To accurately measure free period, one must disconnect all mechanical damping. Initial tests measured free period by digitizing the waveform, then manually measuring the amount of time that transpired between the peaks by counting several oscillations and using a simple stopwatch. This has been the standard method for determining free period for almost a century. It is still the primary method for determining free period in many networks. The trouble is that this method is susceptible to inaccuracies that are the result of the stopwatch and the human eye. Our initial tests would count the exact number of samples that transpired between several peaks to enable us to determine free period to approximately +/-0.1 Hz. As our testing methods improved, we increased the accuracy of this measurement by using signal processing techniques such as frequency spectrum analysis to identify and precisely measure the oscillation frequency (Figure 17). The use of frequency spectrum analysis greatly improved the calculation accuracy of free period (Figure 18), and we integrated the technique into a python program to automatically calculate free-period frequency using a Fast Fourier Transform (FFT) algorithm. This method of determining free period was created shortly after the proof of concept experiments were completed. Mechanical damping ratio is not yet included within the software calculations, but our studies have shown that for most instruments, the effect on resonance frequency is negligible (See section 6.1.8.4). Thus, the accuracy of the free period calculation can now be estimated to within 1.4 % or, +/-0.03Hz (See sections 6.1.3 and 6.1.8.1).

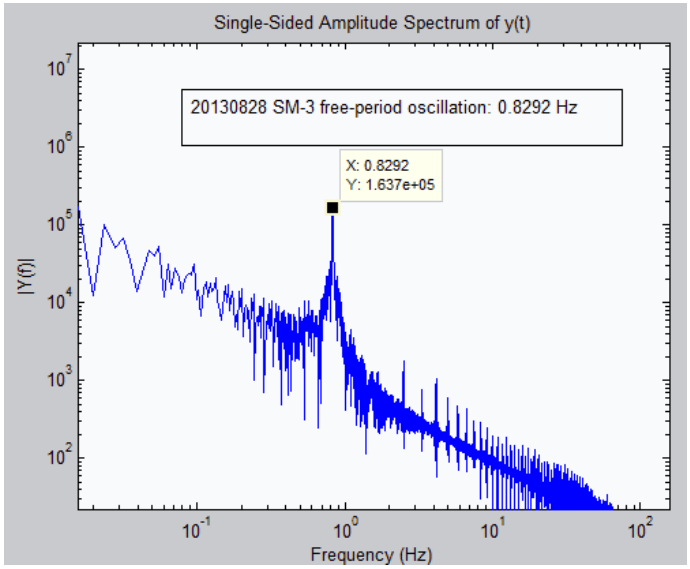

Figure 17: Calculation of free period by using frequency-domain FFT signal analysis.

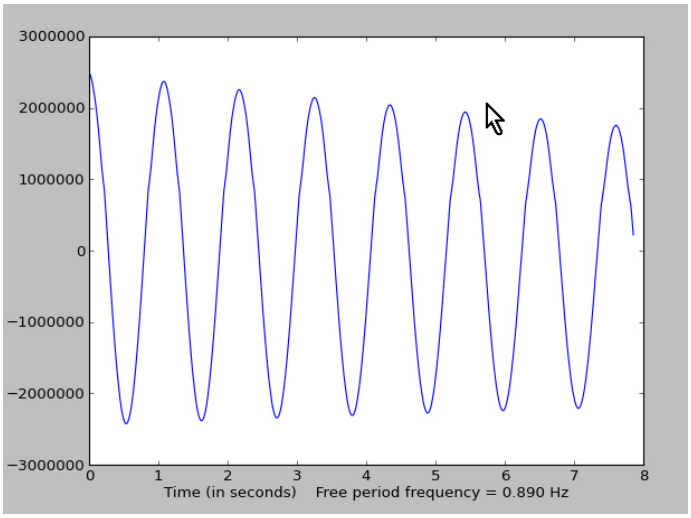

Figure 18: The automated free-period calculation using frequency-domain FFT signal analysis.

5.3 Step 3: Measuring the Electro-mechanical Damping Ratio

The Electro-mechanical damping ratio is a product of both the electronic damping circuit within the seismometer, as well as the electronic damping that occurs as the signal coil interacts with the input impedance of the digitizer (Figure 9). Therefore, it is important to measure damping ratio with the digitizer that is used for routine station operations. We initially measured damping ratio by hand, using spreadsheets but discovered that the damping ratio changes significantly, depending on the amplitude of the signal, and the overshoot number Zn. A damping ratio analysis program was therefore created to automatically determine multiple damping ratios from each subsequent overshoot in the damping impulse and calculate a mean damping ratio that represents the damping within the circuit (Figure 19).

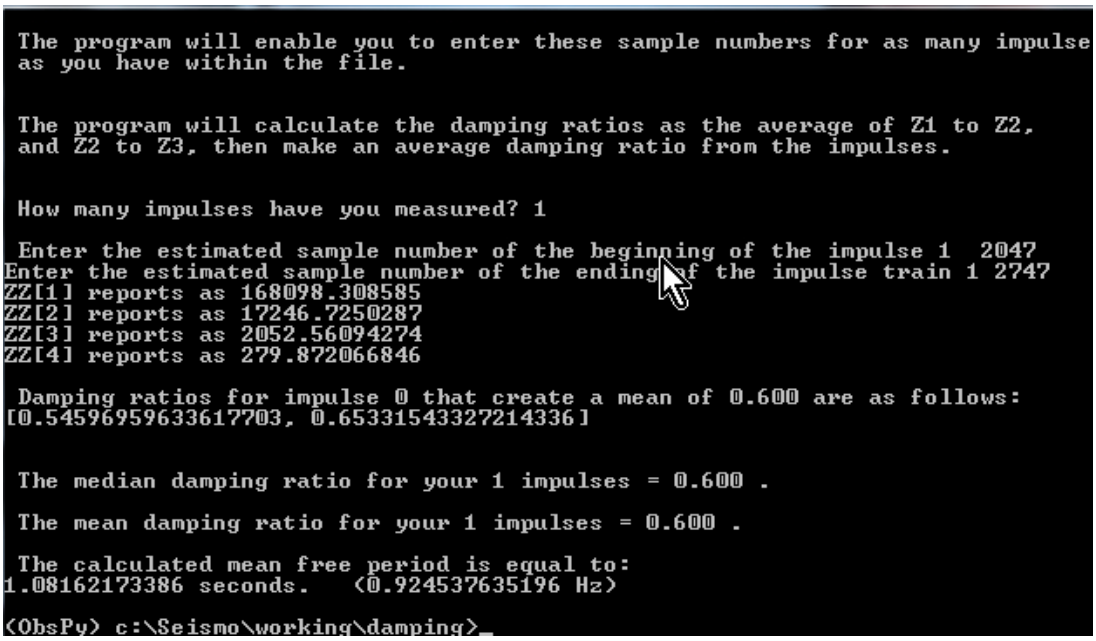

Figure 19: Damping ratio calculation program results.

The estimated accuracy of the damping ratio is still highly dependent on providing the instrument with a clean damping ratio impulse. In many cases, the impulse is created by hand-tapping the armature of the seismometer. The software requires clean releases on the impulse and requires a long enough interval between impulses so that the software can find the "at-rest" position. If either of these conditions are not met, the software has difficulties in calculating a stable damping ratio. Care is therefore required when generating the impulses. A statistical study of damping ratio accuracy indicates that a good representation of damping ratio usually requires an average of three to five impulses (See Chapter 6.1.8.1).

5.4 Step 4: Sine Sweep the Seismometer with the Signal Generator

Once the characteristics of the instrument and data acquisition are known, it is possible to determine ground motion based on mass motion when the seismometer mass is excited with a stationary sinusoidal signal. Amplitude stability is not as important as is frequency stability, because although changes in amplitude cause a deviation in mass velocity, it also causes an equal change in signal coil voltage output, so that amplitude deviations cancel out. Frequency deviations are a much greater concern, for they result in changes in the signal coil sensitivity when signal processing. Most Electro-mechanical seismometers that are still used at regional networks are "short period" instruments with passband frequency sensitivity between 0.1 Hz and 50 Hz. We assume that the instrument exhibits a flat response above about 10 Hz and thus have limited our testing to frequencies between 0.1 and 10 Hz. The chosen frequency band is where the laser position system has enough resolution to provide reasonably accurate mass displacement measurements.

5.4.1 Determining the Frequency of each Break Point

The ground motion from mass motion equation (Equation 5) is solely dependent on the free period, damping ratio, and the excitation frequency of the system. Thus, we need to determine the frequency of the signal used to excite the ground motion. By constraining the seismometer mass excitation to a single sine function that dwells upon a single frequency, we can directly derive the ground motion with simple math. The sine sweep will generate a series of coil sensitivities, but most curve profile changes occur nearest the free period frequency of the instrument. Therefore, to accurately resolve the curve shape, we concentrate our measurement points near the resonance frequency. The actual chosen measurement frequencies are not critical, as long as they remain stable during the data acquisition phase. The dwell time at each frequency should be no less than sixty seconds, especially at periods greater than one second. The analysis software uses a FFT signal processing algorithm to precisely calculate the primary frequency of the signal. Once the battery of excitation frequencies are completed, a separate digital file for each frequency is created for processing each coil sensitivity measurement point.

5.5 Processing the Sine Data to Derive Instrument Sensitivity Curve

The instrument sensitivity Is(ω) as a function of frequency is given by equation 10. In order to derive instrument sensitivity at each frequency, we divide the signal coil voltage by the derivative of ground motion.

$$Is(\omega) = \frac{Vsignal}{\frac{dx}{d\omega}}$$

Equation 10

Where,

Vsignal = Voltage from the signal coil

$\frac{dx}{d\omega}$ = Derivative of measured ground displacement at frequency ω, expressed in meters/sec.

5.5.1 Creating the Calibration Curve

We assemble the entire calibration curve of the instrument by measuring a series of sinusoidal excitations at discrete frequencies throughout the passband of the instrument. By calculating instrument response at each frequency, we then interpolate between each measurement to re-create the whole-system response curve. This amplitude versus frequency curve determines the voltage sensitivity of the instrument over its entire passband (Figure 14).

5.5.2 Processing Methods: Full Derivative vs. Fourier Transform

When we first started researching the viability of the mass displacement method, we processed data from each frequency breakpoint by calculating both integral of the coil voltage, as well as derivative of the ground displacement, then averaging the results of both calculations to determine the instrument sensitivity at that frequency. Unfortunately, this method, though mathematically accurate, proved to be rife with complications. The waveforms had to be carefully tracked to eliminate dc bias problems by calculating a running weighted average, or else problems with the integral calculations would result. Derivative calculations proved problematic whenever the signal approached a zero crossing. These problems were eventually solved, although the processing alrorithm was very time intensive. The full derivative method initially required several days of hand calculation when using Microsoft Excel when proving the initial methodology. A move to the programming language Python reduced the processing time to a matter of about 17 minutes processing time per calibration. However, this was still an unacceptable amount of time for calculating the instrument response. It became obvious when demonstrating the method to experts in Obninsk, Russia that we needed a faster method. To that end, we switched the signal processing algorithm from the time domain to the frequency domain by employing a FFT signal processing algorithm.

The FFT algorithm converts the signal from the time domain to the frequency domain, and describes each waveform as a series of statistical “bins full of energy”, each of which represent a discrete

frequency band. The beauty of this method is that the dc bias problems are no longer of concern our calculation, because the energy representing the dc signal gets piled into the lowest bin. Any noise, such as a 60 Hz hum from an AC power source, gets placed in a separate frequency bin. The energy for the signal of interest gets conveniently placed within its own bin. Thus, processing for the primary frequency becomes a matter of selecting the appropriate frequency bin and tallying up the energy. This is done for both the seismometer output signal (representing voltage), and the laser position sensor signal, which is corrected to reflect equivalent ground motion. Since the FFT is based on a mathematical Taylor series, the energy is assumed to represent a pure sinusoidal signal. Thus, all that is necessary to convert the ground displacement into ground velocity, is to multiply the energy by $2\pi f$ (See Equation 7). By comparing the signals in the frequency domain, the math is greatly simplified, and there is no need to laboriously process integrals and derivatives sample-by-sample. The processing time has been reduced from 17 minutes to less than 10 seconds. Although this is a radical change in how the sensitivity of the instrument is calculated, the final result remains unchanged, with less than three percent deviation at any given frequency break point (Figure 20, Table 4).

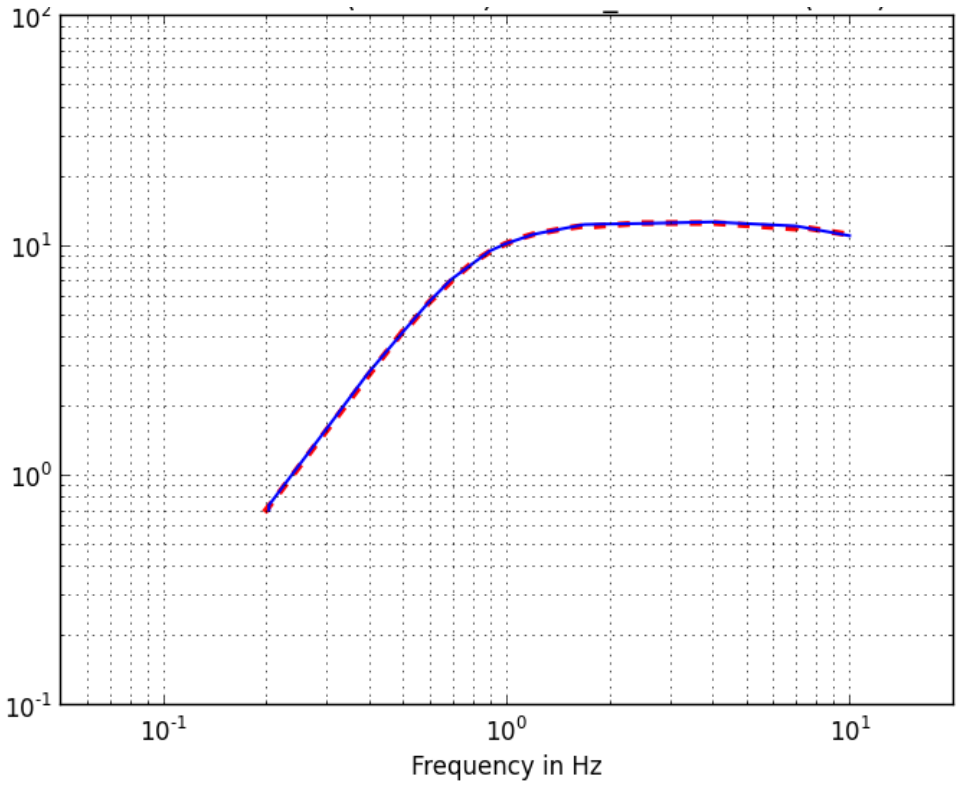

Figure 20: Response calculation: Mass displacement derivative vs. FFT-rms methods. Vertical units are V.sec/meter. The full derivative is depicted as a red dash whereas FFT-rms is depicted in blue. There is negligible difference in calculation of sensitivity between the two methods.

```
% deviation between response calculation of :
 Original derivative calculation vs. new FFT_rms calculation method

 Albuquerque data, 29Aug2013, SM3 seismometer.
At Frequency = 0.2 Hz, Derivative / FFT_rms deviation = 1.97 %
At Frequency = 0.4 Hz, Derivative / FFT_rms deviation = -0.23 %
At Frequency = 0.5 Hz, Derivative / FFT_rms deviation = -0.21 %
At Frequency = 0.6 Hz, Derivative / FFT_rms deviation = 0.97 %
At Frequency = 0.7 Hz, Derivative / FFT_rms deviation = -0.19 %
At Frequency = 0.8 Hz, Derivative / FFT_rms deviation = -1.18 %
At Frequency = 0.9 Hz, Derivative / FFT_rms deviation = 0.99 %
At Frequency = 1.0 Hz, Derivative / FFT_rms deviation = 0.22 %
At Frequency = 1.2 Hz, Derivative / FFT_rms deviation = 0.04 %
At Frequency = 1.7 Hz, Derivative / FFT_rms deviation = 2.42 %
At Frequency = 1.9 Hz, Derivative / FFT_rms deviation = 1.45 %
At Frequency = 2.5 Hz, Derivative / FFT_rms deviation = -0.35 %
At Frequency = 4.0 Hz, Derivative / FFT_rms deviation = 0.98 %
At Frequency = 7.0 Hz, Derivative / FFT_rms deviation = 2.55 %
At Frequency = 10.0 Hz, Derivative / FFT_rms deviation = -1.13 %
```

Table 4: Percent deviation between full-calculation of ground motion derivative vs. rms of FFT.

5.6 Validating Against a Reference: Testing in Obninsk, Russia

The Mass Displacement Tracking (MDT) calibration method was tested against the official calibrations at the metrology laboratory of the GSRAS in Obninsk Russia in July, 2014. The staff provided two new SM-3 seismometers in a blind test for us to calibrate (Figure 21). Each seismometer was calibrated using the MDT method. GSRAS then compared the calibration to their official calibration in terms of calculation of free period, damping ratio, and sensitivity. The GSRAS calibration is created on a vibration table by measuring the signal coil output voltage, vibration frequency, and table displacement via laser-based displacement measurement system. The table displacement represents ground motion. This test is performed at three discrete frequencies: 5, 7, and 9 Hz. GSRAS then manually converts each table displacement measurement to velocity and hand-calculates the sensitivity of the instrument within its passband. GSRAS assumes that the instrument will perform predictably according to the equations of forced motion, and uses the measurement of damping ratio and free period in order to calculate the poles and zeros of the seismometer. The MDT method also relies upon these same equations: However, rather than directly measure ground motion (as performed in the GSRAS test), we calculate ground motion based on knowledge of the mass motion, damping ratio, and free period. Sensitivity values within the passband for both calibration methods, performed independently from one another, resulted in measurements within one percent of one another (Table 5; Figure 22).

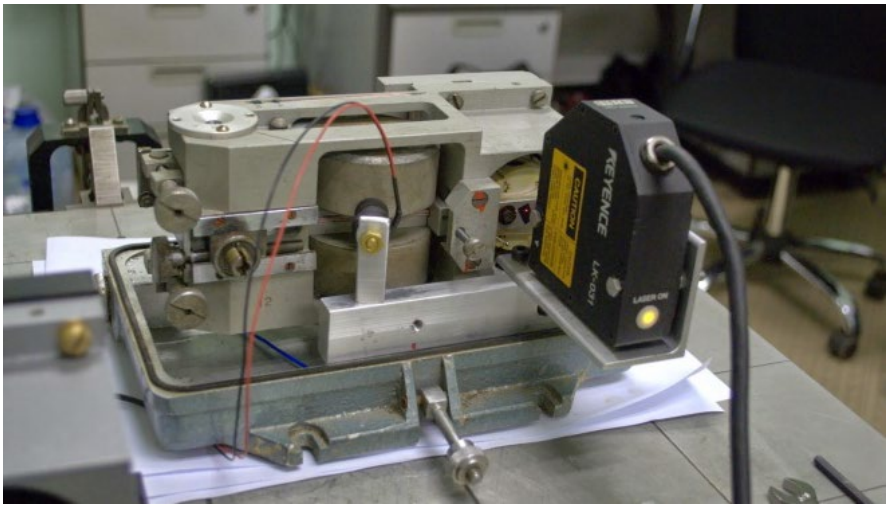

Figure 21: SM-3 horizontal at GSRAS, resting on shaker table but calibrated with Keyence laser.

Seismometer	Free Period (Hz)	Damping Ratio	MDT Sense V•sec/m	OBN Sense V•sec/m	%difference
SM-3 SN001	0.487	0.775	177.7	177.8	0.06
SM-3 SN002	0.491	0.689	180.8	181.5	-0.4
VEGIK SN439	0.998	0.538	88.5	89.0	0.6

Table 5: Sensitivity difference, MDT calibration vs. official GSRAS calibration.

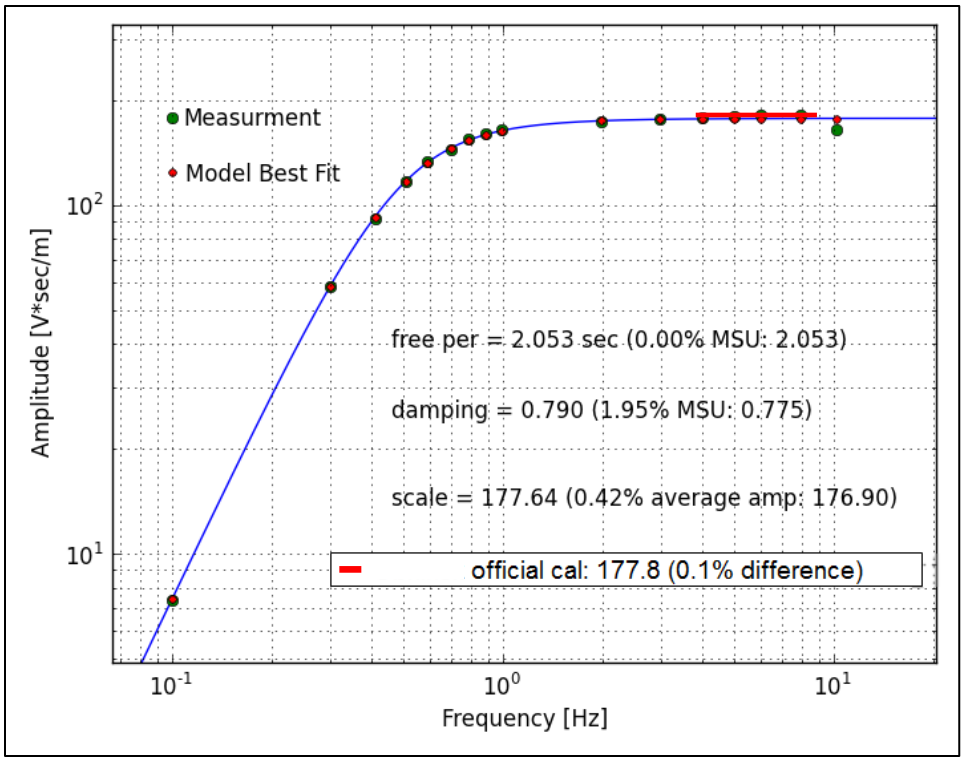

Figure 22: SM-3 horizontal (SN-001) calibration (green dots) versus GSRAS official calibration (Red line) sensitivity using the vibration table. GSRAS tests instruments with sine sweeps at only at 5, 7, and 9 Hz. Sensitivities correlate within 1 %.

5.7 Translation of Instrument Response to Poles and Zeros

The calibration should be described in a 'standard' format in order to be useful for the general seismological community. The format that is most often used is to describe the non-linear curve in terms of a 'poles and zero' format (Table 6). One particular form is called the 'SACPZ' file for use with the seismic processing program SAC. This file yields the essentials of the instrument response, namely the amplitude, and two* poles & zeros (in units of 2π radians/second) that determine the size and shape of the curve.

This file can then be translated into other formats as necessary, such as a dataless SEED file. The advantage of the SACPZ format is that it is supported in ObSpy (Beyreuther *et al.*, 2010). Obspy is a seismic analysis software package that we used for curve-fitting the existing calibration curve to poles and zeros using the Python programming language. Hans Hartse of Los Alamos National Laboratory provided code that utilizes ObSpy to fit the system response curve to the nearest SAC poles & Zeros description (Figure 23).

It is important that the calibration process include a description of the entire channel, from sensor response, to digitizer gain, to even the station name and coordinates. There exists a response description in the form of a "dataless seed file" that is generally accepted throughout the greater seismological community. A final portion of the calibration should therefore be the generation of a station calibration description that can be attached to all station data assets. Once completed, the result should be data holdings that are useful for advanced seismic research.

*SAC requires an additional "third" zero be declared to properly handle data files.

ZEROS 3
POLES 2
-2.268519e+00 -3.746037e+00
-2.268519e+00 3.746037e+00
CONSTANT 4.063795e+02

Table 6: Initial calibration of SM-3 at Albuquerque Seismological Labs, Albuquerque, NM, as expressed in "SACPZ" data format, representing instrument response as a function of sensitivity constant, poles & zeros.

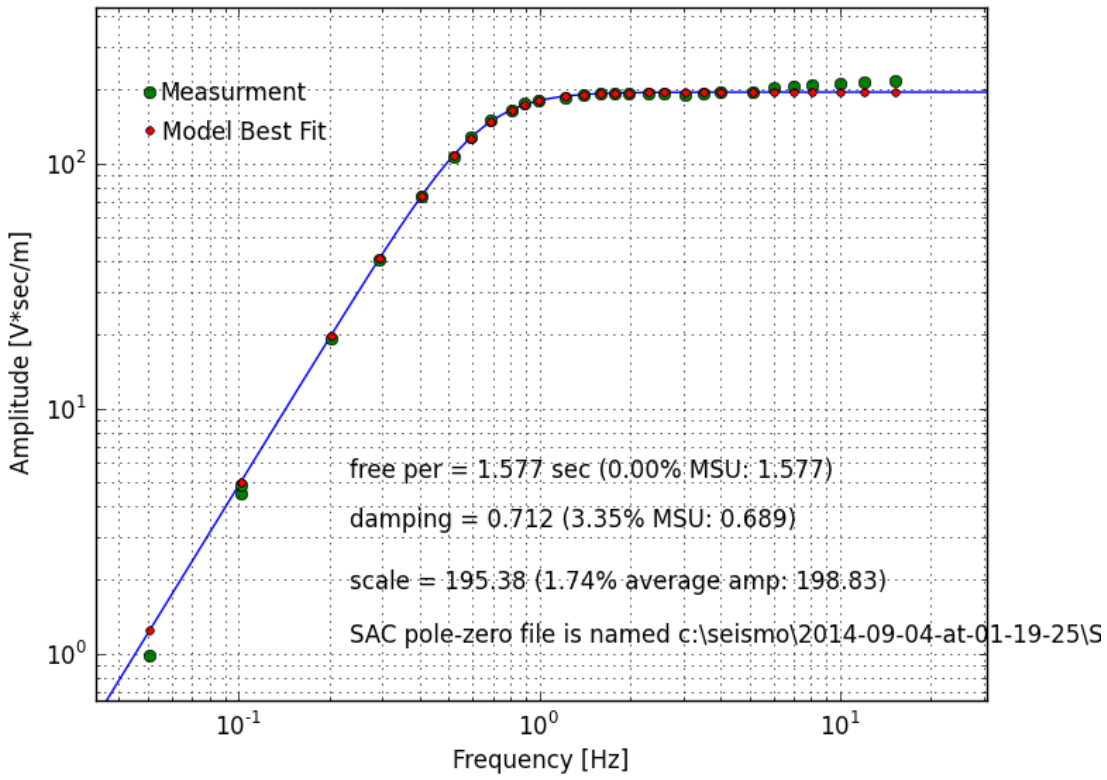

Figure 23: Calibration of a test SKM seismometer (green dots) with resulting poles and zeros response curve in blue. Red dots are the intersection of the poles and zeroes model to the frequencies under test.

CHAPTER 6: ESTIMATION OF CALIBRATION UNCERTAINTIES

How accurate is a measurement of calibration? That is a fair question, as no measurement, no matter how precise, will be perfect. There will always be some amount of measurement uncertainty, be it +/- 0.1 %, 1 %, or 10 % of the measure. In the case of the measurement of the seismometer, even environment such as temperature and barometric pressure will play a small (but probably measurable) part. However, this chapter deals with the more easily quantified uncertainties, to approximate the answer of "how close are we to the true response?" Even so, it is best to understand that uncertainty is a statistical quantity, that can be expressed as a function of some multiple of standard deviation. This chapter uses 2X standard deviation, unless otherwise stated.

The accuracy of the calibration is dependent on multiple variables, some of which are defined as published constants, and others that are dynamically measured during the calibration process. The MDT method relies upon the fundamental equation of forced motion that is essential to all Electro-mechanical seismometer models and calibration methods, and therefore is dependent on accurate measurement of both resonance frequency and damping ratio. In this chapter, we examine each variable and make an estimate of its uncertainty and how it affects the overall calibration as a function of frequency. We then add up these uncertainties to produce a plot of measurement uncertainty versus frequency. We then use an empirically derived set of calibration data, and analyze the scatter of the measurement points, to produce an estimate of overall percentage uncertainty as a function of frequency.

6.1 Variables that Influence Sensitivity at any Given Frequency

The calculation of sensitivity (as a function of frequency ω) is dependent on eight variables (Equation 11). Two additional variables also influence sensitivity by way of the variable GMCORRECT, which depends on both resonance frequency and damping ratio as previously expressed in equation 5.

$$\text{Sense}(\omega)\left[\frac{Volts*Seconds}{Meter}\right] = \frac{\text{Coil voltage [Counts]}}{1} * \frac{[Volt]}{VcADC[Counts]} * \frac{[Seconds]}{\omega} * \frac{1}{Displacement[Counts]} * \frac{Laser\ ADC\ cal[Counts]}{[Volt]} * \frac{[Volt]}{Lasercal[Meters]} * \frac{1}{LCAL} * \frac{1}{GMCORRECT(\omega)}$$

Equation 11

Where,

Coil Voltage = Root Mean Squared (RMS) voltage at frequency ω, expressed in digitizer counts.

VcADC = Digitizer channel gain monitoring coil voltage in Counts/Volt.

ω = Frequency of excitation signal being analyzed in Hz.

Displacement = RMS of mass displacement (in meters) at ω, in digitizer Counts.

Laser ADC cal = sensitivity of digitizer channel for laser displacement in Counts/Volt.

Lasercal = The gain of the laser measurement device in Meters/Volt.

LCAL = ratio of laser measurement point to pendulum center of mass (Equation 8).

GMCORRECT(ω)= Ground Motion amplitude correction factor to resolve ground motion from mass motion as a function of excitation frequency (Equation 5).

Given the above variables, the overall measurement uncertainty is therefore a sum of the uncertainties for each variable, that can then be plotted as a function of frequency. Some of these variables have a measurement uncertainty that is constant with respect to frequency whereas others vary in amplitude as a function of frequency.

6.1.1 Coil Output Voltage

Peak coil voltage represents the velocity output of the seismometer as expressed in terms of digitizer counts. Uncertainty of this variable is attributable to sample rate, quantization error of the digitizer and the noise level on the output signal. In order to maintain a good signal to noise ratio, it is important to provide sufficient mechanical excitation energy into the system. In the case of our testing, the digitizer used is a Symmetric Research USB4CH, 24-bit digitizer. The digitizer quantization error is approximately +/-1 microvolt. The noise level, however, is a complex function of frequency, wire length, grounding practices and sample rate that changes significantly, based on hardware and test location. One of the techniques used within our calibration signal analysis code is to analyze the signal coil output in the frequency domain. Rather than use a single period of the signal, many periods within the entire digital record are summed together using a FFT algorithm. By doing so, the energy of the signal coil output at the excitation frequency is isolated, and off-frequency energy from noise is easily discarded. This boosts signal to noise ratio to enable the calibration code to accurately resolve coil signal at very low amplitudes. The limiting factor seems not to be excitation amplitude, but instead excitation frequency: Mass velocity and ground velocity are related through a function of frequency (Equation 5). As excitation frequency decreases (and period increases), mass velocity drops to lower and lower amplitudes relative to ground velocity, resulting in a logarithmic decrease in signal voltage output. Uncertainty of this variable is therefore primarily frequency and especially velocity dependent. In practice, there must exist sufficient mass velocity at the lowest measured frequency to provide a voltage output that is greater than the noise floor of the digitizer. The measurement of this uncertainty cannot be expressed as “n” percent because it is dependent on the unique qualities of the digitizer used, along with the noise floor, and the velocity of the signal coil. For the purposes of this thesis, the uncertainty estimation of peak coil voltage is convolved within the empirical calibration uncertainty measurement tests found within section 6.7.

6.1.2 VcADC Digitizer Channel Gain

The digitizer channel gain is a scalar that directly affects calibration regardless of amplitude or frequency. It is expressed either in terms of microvolts per count, or counts per volt. For the purposes of this thesis, it is assumed that the digitizer channels have been calibrated. A typical 24-bit digitizer can be successfully calibrated to one or two parts in a thousand: i.e. 0.2 % or less.

6.1.3 Frequency Under Study (ω)

Seismometer excitation frequency affects the derivation of ground motion from mass motion. The way we calculate frequency is by convolving the time-history data into the frequency domain. The distribution of energy is then 'binned' into discrete frequency segments of width Δω. The excitation frequency is then identified by determining the center peak of the main power impulse. This center frequency represents the excitation frequency. The measurement uncertainty of ω is represented by the width of a single bin in the frequency domain and is determined by FFT windowing segment size and sample rate using the following relationship:

$$\text{Frequency Resolution} = \frac{Sample\ Rate(Hz)}{segment\ size}$$

For example, when testing the calibration method with the Symmetric Research digitizer, we typically set our sample rate to 130.2 samples/second (The odd sample rate is a function of this digitizer model), and our FFT windowing segment size is set to no less than 4096 samples. Thus, Δω = 130.2 Hz/4096 = 0.032 Hz. Assuming that the true frequency lies +/- 1 bin from the peak, the measurement uncertainty should be +/- 0.03 Hz in this example.

6.1.4 Mass Displacement

The mass displacement used for the calibration process is calculated as the RMS of mass displacement at frequency ω , as expressed in digitizer counts. Mass displacement is measured via a Keyence laser position sensor. It is frequency dependent, as well as dependent on quantization error, both from the digitizer itself and from the Keyence position sensor, that converts a digital measurement of displacement into an analog voltage. This analog voltage however, is not continuous, but is quantized in 'steps' representing approximately one micron per step. Most of the Keyence position sensors are configured to output 1 volt per millimeter, or, 1 millivolt per micron. Therefore, the digitizer will measure displacement in 'steps' of 1000 microvolts per micron. Quantization also occurs at the digitizer: As an example, the digitizers used in our research (Symmetric Research USB4CH) typically feature a gain of 0.954 microvolts per count. Therefore, a 1000 microvolt step from the laser position sensor will result in a 954 count step for each observed micron of displacement. Thus, measurement uncertainty is likely a function of the resolution of the laser position sensor more-so than the digitizer. Therefore, mass displacement uncertainty can be safely assumed to be within 1 micron in the case of the LK-31 laser position sensor, or 0.5 micron for the LK-G32 sensor. Mass displacement uncertainty does, however have a signal frequency dependence: The laser can accurately track displacements from dc to about 10 Hz. Anything greater results in a roll-off of the digital-to-analog voltage output from the laser. Sufficient mass displacement is also difficult to maintain at frequencies higher than 10 Hz, as this requires ever-increasing amounts of energy from the excitation coil. Since accurate mass displacement tracking is critical to this calibration method, calibration excitation frequencies should be limited to 10 Hz or less.

6.1.4.1 Minimum Mass Displacement for an Accurate Calibration:

Mass Displacement has been shown to be one of the limiting factors within the calibration methodology in terms of accuracy, especially at higher frequencies where it takes more energy to move the seismometer mass: It is quite easy to fall to a level of displacement that is below the laser position measurement resolution. Therefore, excitation of the mass must result in mass displacement that is guaranteed to exceed the laser minimum resolution in order to yield accurate sensitivity. Additionally, the laser position measurement system appears to lose its dc bias with time when experiencing sinusoidal excitation and can vary its peak measurement by up to one micron. Therefore, the minimum mass displacement should be about 100 times this one-micron variation, or, 100 microns if one wishes to keep the sensitivity calculation to within one percent.

6.1.4.2 Observed Limitations of Laser Position Sensor as a Function of Frequency

The Keyence LK-G32 laser position sensor is a useful tool for the calibration because it is capable of accurately measuring mass displacement to within 0.5 micron. It has been repeatedly tested and shown to provide a linear response from +/-5mm. However, when mass motion becomes dynamic, the laser seems to lose track of its position, which manifests itself as a slow change in dc bias (Figure 24). DC bias shifts in and of themselves are not a problem, because all amplitude calculations are performed in the frequency domain, where it is easy to ignore the energy that is found outside of the primary excitation frequency. The problem is that as dc bias moves, so does the peak-to-peak amplitude of the signal. Figure 24 shows the raw time-history of a portion of the sensitivity scatter test of section 6.2.2. In it, frequencies from 7 through 10 Hz are shown. During this test, the excitation voltage and current is held constant, thus the force imparted into the system via excitation coil also remains constant. As excitation frequency increases, physical mass displacement decreases, as does mass velocity. However, since mass displacement and seismometer mass velocity are mathematically related, the decreases should always remain

proportional to one another. If the problem was one of overheating of the excitation coil, or a problem with the signal generator itself, it would be observed as a change on the seismometer signal as well as the laser position sensor. The Seismometer signal remains constant and only changes when moving to a different frequency, as is expected. The laser however, loses signal amplitude as a function of time and displacement offset. The amount of this amplitude loss appears to fall between 500 and 1500 digitizer counts (Table 7). This amounts to an amplitude variance of 1 to 1.5 microns. Unfortunately, at frequencies above 5 Hz, the mass displacement drops below 40 microns, decreasing further with higher frequency. Thus, as actual measured displacement gets smaller, the one micron loss in the peak measurement results in increasing inaccuracy. At 10 Hz, the system displacement is less than 10 microns. This is why, when there is a one micron deviation in laser sensitivity, the calculation of seismometer response can vary by as much as nine percent. Keyence corporation has not yet provided an explanation for why sensitivity is a function of both time and dc offset.

Therefore, the calibration hardware (Specifically, the excitation coil circuit) should keep the displacement above 100 microns (0.1 mm) at all measured frequencies to minimize the adverse effects of laser measurement error.

Frequency (Hz)	Displacement Starting Counts	Displacement Ending Counts	Percent Deviation	Displacement (microns)
0.1	610400	610900	0.1 %	577.4
0.5	639000	641000	0.3 %	605.1
0.7	646000	646000	0.0 %	610.8
0.9	615000	615000	0.0 %	581.5
1.0	578300	578000	0.1 %	546.6
2.0	186500	186000	0.3 %	176.1
3.0	118000	117000	0.9 %	111.1
4.0	65000	64500	0.8 %	61.2
5.0	41000	40900	0.2 %	38.7
6.0	29000	31000	6.7 %	28.4
7.0	21800	21400	1.9 %	20.4
8.0	16500	16000	3.1 %	15.4
9.0	12100	11500	5.1 %	11.2
10.0	9400	8900	5.5 %	8.7

Table 7: Dwell test. Laser position sensor channel with beginning and ending raw counts for each frequency representing displacement, percentage deviation of displacement, and peak mass displacement for each frequency.

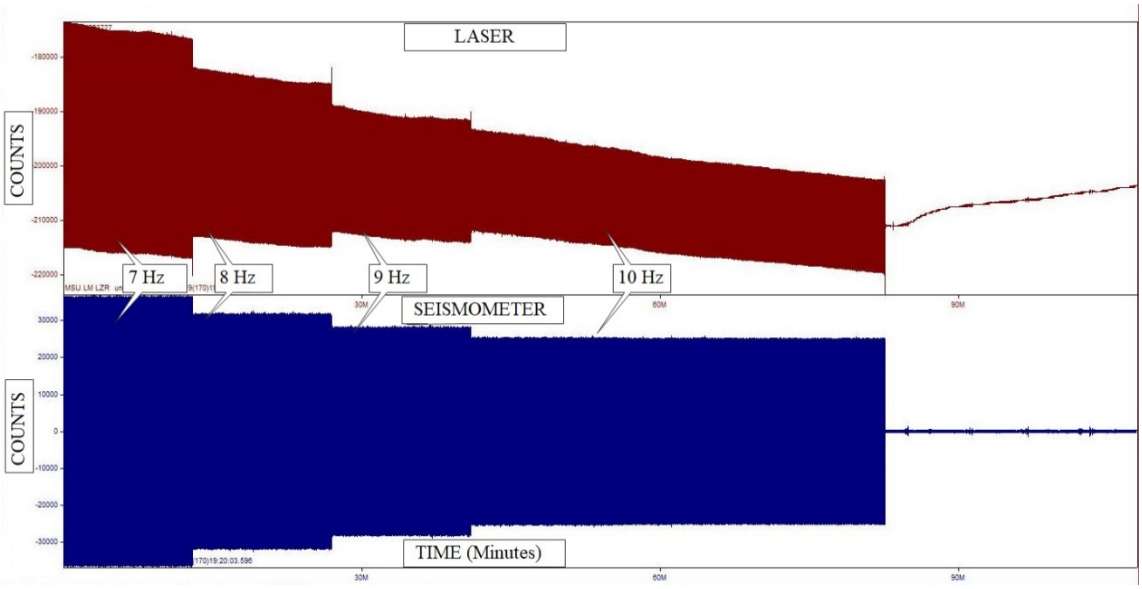

Figure 24: Dwell Test illustrates sensitivity 'droop' of laser position sensor with increased excitation frequency from 7-10 Hz vs. time. Laser in red and seismometer signal is in blue. The laser position sensor dc bias drifts as a function of time. Additionally, the peak-peak amplitude declines as dc bias changes, while seismometer signal coil voltage remains steady.

6.1.5 Laser ADC Digitizer Channel Gain

Part of the laser output measurement uncertainty is the digitizer gain, as expressed in terms of counts per volt. Like the seismometer digitizer gain, this scalar value (which is not dependent on excitation frequency) is dependent on an accurate calibration of the digitizer channel and can be reliably held to within 0.2 %.

6.1.6 Lasercal

The laser analog to digital converter (ADC) measurement uncertainty is not only dependent on the gain of the digitizer, but also the gain of the laser position sensor. There are several models of laser position sensors in use. The two models used for this research are the Keyence LK-31 and the Keyence LK-G32. Both feature an adjustable gain. Therefore, it is important to calibrate the laser position sensor. All sensors used for this research have been calibrated using a known displacement and a high-quality digital caliper. First, the laser position sensor is re-programmed to its default gain setting. The caliper is then stepped in 0.5 mm increments from -5.0 mm through +5.0 mm in order to optically characterize both the gain and the linearity of the laser position sensor. A precision volt meter tracks the analog voltage output to the nearest 100 microvolt. A “best-fit” curve of the gain is computed from these twenty points to arrive at a measurement of gain in terms of volts per millimeter for the laser (Figure 16). This value is termed “lasercal” and is considered to be accurate to within one part in a thousand. Because it is possible to adjust the gain of the laser position sensor, it is important that the user periodically re-check the gain. Once calibrated, the measurement uncertainty of the laser signal may be considered to fall within 0.1 %, or twice the minimum resolution of the laser position sensor, whichever is greater.

6.1.7 Laser Calibration Constant (LCAL)

The mass moment is defined as the distance from the pivot point to the center of oscillation within the pendulum (Figure 2). It is this point where seismometer mass displacement can be related directly to physical ground motion. Unfortunately, it is sometimes impossible to fixture the laser position sensor to this point. LCAL is the ratio of the mass moment divided by the distance from the pivot point to the laser measurement point, where relative mass displacement is measured (Equation 8). Systems in which the measurement point are farther along the pendulum arm than the mass moment will measure a displacement that is higher than the actual mass displacement. Thus, it must be geometrically accounted for with the scalar LCAL. For pendulum-based seismometers, such as the Russian SKM or SM-3, this ratio is less than one because of the difficulty in mounting the laser at the sensor's pendulum mass center. For seismometers such as the Geotech S-13, the pivot point and center of oscillation, and laser measurement point are colinear, resulting in an LCAL of one. It is difficult to properly asses the actual distance from fulcrum to mass center in the pendulum based Electro-mechanical seismometer, but it can be derived in three different ways: By disassembly of the seismometer in order to measure the effective mass moment, by locating the center of oscillation of the seismometer on a vibration table, or by inferring the LCAL by co-locating the test seismometer against a known reference seismometer with a known good calibration. LCAL should not appreciably vary from seismometer to seismometer within a given model type. Even if it does, the percentage of change in ground motion is not significant for small changes in mass moment due to manufacturing deviations. This scalar is independent of frequency and affects the calibration sensitivity equally at all excitation frequencies.

6.1.8 GMCORRECT

The ground motion correction factor (GMCORRECT) utilizes the equations of forced motion to calculate ground motion based on the amplitude of mass motion. It is a function of excitation frequency ω, damping ratio (h) and resonance frequency (ω_o) (Equation 5). The calculation of GMCORRECT directly influences the uncertainty of the calibration as a function of these three variables. Its measurement uncertainty has been empirically estimated for this thesis by analyzing the measurement uncertainties of ω, h, and ω_o.

6.1.8.1 Damping Ratio Measurement and Accuracy Estimations

The precise measurement of damping ratio plays a direct role in the accuracy of the calibration. Therefore, the goal should be to measure the damping ratio to the highest degree possible, within reason. A goal of one percent was arbitrarily chosen as providing a good representation for acceptable calibration accuracy. An empirical study of forty-one electrically induced damping ratio pulses was performed to determine the minimum number of pulses necessary to converge on a solution that is within one percent of the actual damping ratio (Figure 25). Amplitudes were held to modest levels to ensure seismometer mass displacement stayed within a reasonable operating range for teleseismic signals: The peak amplitude for the initial rebound impulse was measured at a typical value of about 250 microns (Figure 26). Multiple impulses enable a more accurate measurement of damping ratio. Impulses without a clean release of seismometer mass should be discarded. The use of averaging multiple impulses improves accuracy, depending on the signal quality of the impulse. The idea of using multiple impulses is to ‘average’ out deviations that might occur due to inconsistencies with impulse size, clean-release of the mass, or due to a noisy environment that affects the overshoot peak and dc bias because of background seismic signal. In the case of this particular study, the first eight impulses were inconsistent in terms of amplitude as the operator familiarized himself with the electromagnet that served as means for inducing a mechanical offset

into the seismometer pendulum. Once familiarized, the push-button that energized the electromagnet was applied consistently for a clean release for the remainder of the test. The initial inconsistency, however, lends insight into the type of variation one might see in a damping ratio measurement because of varying impulse amplitudes or a novice operator. In the case of this study, nearly all damping ratio impulses fall within one percent of the nominal value of 0.7046 (Figure 27). The standard deviation of the 41 impulses was 0.0036, or within 0.52 % of the nominal value. This likely represents the best-case scenario for the damping ratio calculation algorithm of our software. When we look at the first eight impulses, that varied in terms of signal amplitude, the average measured damping ratio rises to 0.8 % of the 41-sample nominal. It is likely that a 'best practice' should be to use three to five "clean" damping ratio impulses to reduce inaccuracies arising from varied amplitudes.

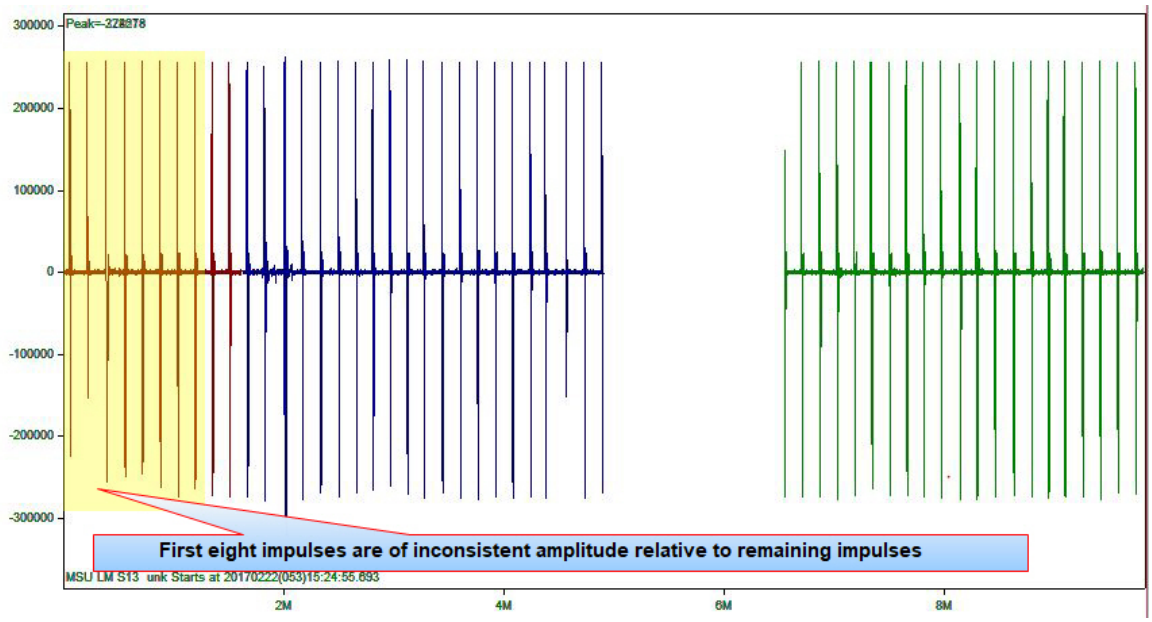

Figure 25: Fourty-one damping ratio impulses to study consistency of damping ratio measurements. Measurement units are in counts. First eight impulses vary in terms of amplitude., but the rest are 'clean' as operator becomes more consistent with applying the impulse. 328,000 counts represent approximately 250 microns of pendulum displacement.

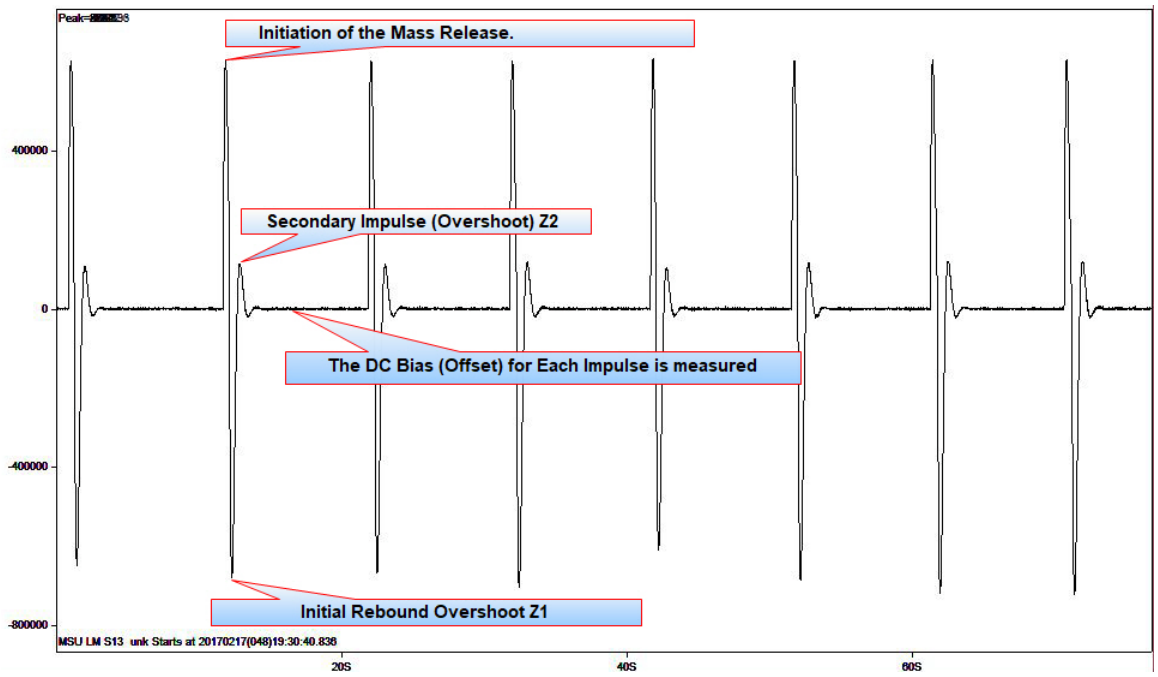

Figure 26: Sample damping ratio impulse train. Y axis is listed in counts.

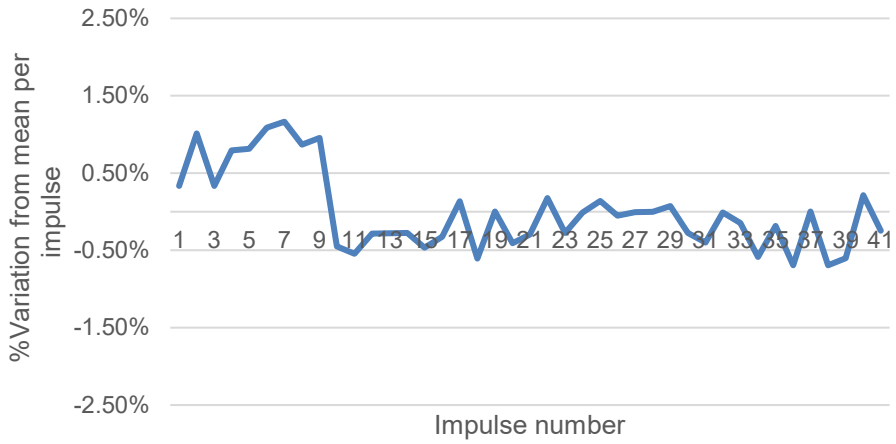

Figure 27: Percent variation of damping ratio measurement from the nominal for 41 impulses, where nominal damping ratio = 0.705. The standard deviation is 0.52 %. Vertical axis represents percent deviation from the mean, whereas horizontal axis represents the impulse number.

6.1.8.2 Damping Ratio (h) Empirical Estimation of Measurement Accuracy

The damping ratio is likely to be the variable with the most influence on the accuracy of calibration. An empirical study of the of how calibration is influenced by damping ratio was performed on a Geotech S-13 seismometer. The seismometer damping ratio and resonance frequency were first carefully measured to determine their nominal values (damping ratio = 0.7245, resonance frequency = 1.017 Hz). Next, the calibration of the S-13 was run three times with a damping ratio set to the nominal value of 0.7245, and -+0.52 % of nominal (0.718 and 0.732 respectively). This target was chosen based on the previous study (Section 6.1.8.1) that demonstrates that the damping ratio calculation standard deviation approaches +/-0.52 % of the actual seismometer damping ratio with just a few summed impulses. When the calibration is run using the nominal, maximum and minimum (+/-0.52 % nominal) damping ratio measurements, (Figure 28) the most amplitude deviation occurs at the resonance frequency as a result. In each case, the total amount of sensitivity inaccuracy occurs at the resonance frequency, to a measured total of +1.06 % for under-reported damping ratios, and -1.04 % for over-reported damping ratios (Figure 29). The effect of damping ratio accuracy on the calibration accuracy rapidly drops as the excitation frequency moves away from the resonance frequency. An under-reported damping ratio will force the seismometer to look more sensitive than it really is, and vice-versa. (Figure 7).

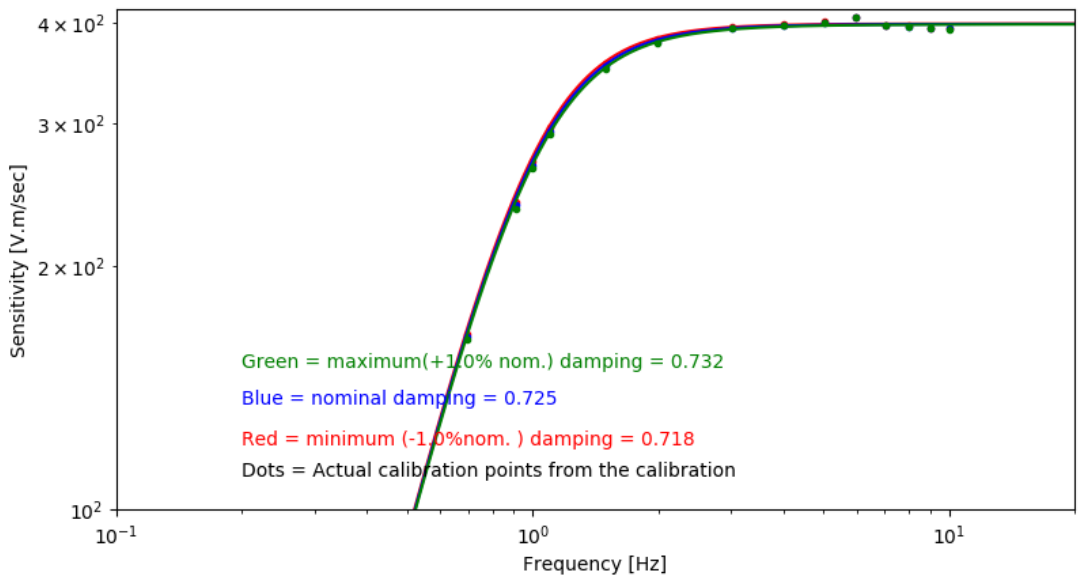

Figure 28: Frequency vs Amplitude curves with three different damping ratios. The curve deviates the most at the resonance frequency when damping ratio is not accurately measured.

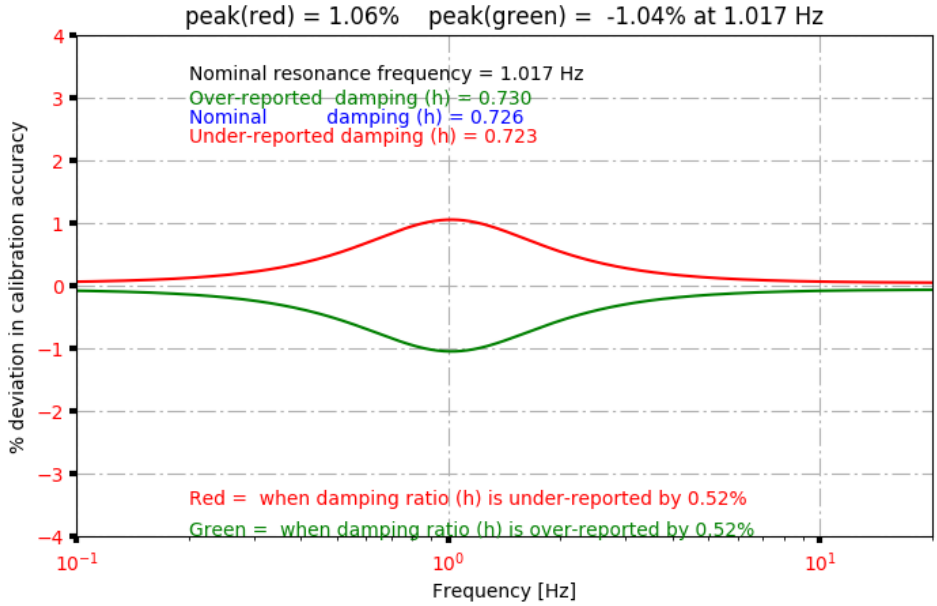

Figure 29: Measured percent deviation from the nominal sensitivity curve as a function of frequency for damping ratios that deviate by 0.52 % of nominal value of 0.726. The peak deviation occurs at the resonance frequency and is slightly higher (1.06 %) when the damping ratio is under-reported.

6.1.8.3 Free Period Empirical Estimation of Measurement Accuracy

Part of the accurate translation of mass motion into ground motion also involves the precise measurement of free period (i.e. resonance frequency) of the instrument. This is accomplished using a FFT and multiple periods within the frequency domain. By convolving the signal into the frequency domain, the whole signal is statistically sampled and binned into energy bins.

6.1.8.4 Deviation in Free Period due to Mechanical Damping Ratio

One uncertainty within the measured calibration is accounting for the difference between observed and true free period of the instrument due to mechanical damping ratio (Described in section 2.3). The calibration software does not currently account for this parameter, because the highest observed mechanical damping ratio of 0.146 is for the S1-P seismometer (Table 2). This results in a deviation of observed free period versus true free period of 1.15 %. The majority of sensors tested feature a mechanical damping ratio typically less than 0.05. The result is that the calibration is altered in terms the location of the sensitivity slope at low frequencies. As an example, with a 1.15 % deviation in free period calculation, the instrument response is altered by a peak value of 2.4 % at the frequencies below the resonance frequency (Figure 30). This represents the 'worst case' that we have found with Electro-mechanical seismometers in the field thus far. A more typical mechanical damping ratio, such as found on the Geotech S-13 is 0.046 that shifts the resonance frequency by only 0.08 %. This results in an observed resonance frequency shift from nominal that is negligible (0.001Hz). Thus, because the observed mechanical damping ratios of the majority of seismometers observed fall below 0.14 (Table 2), the influence of this parameter on the calibration is minimal. Because the effect is negligible, and the necessary coding for integrating this parameter into the calibration software was sufficiently complex, it was deemed unnecessary to include it in the initial calibration software which was part of this study.

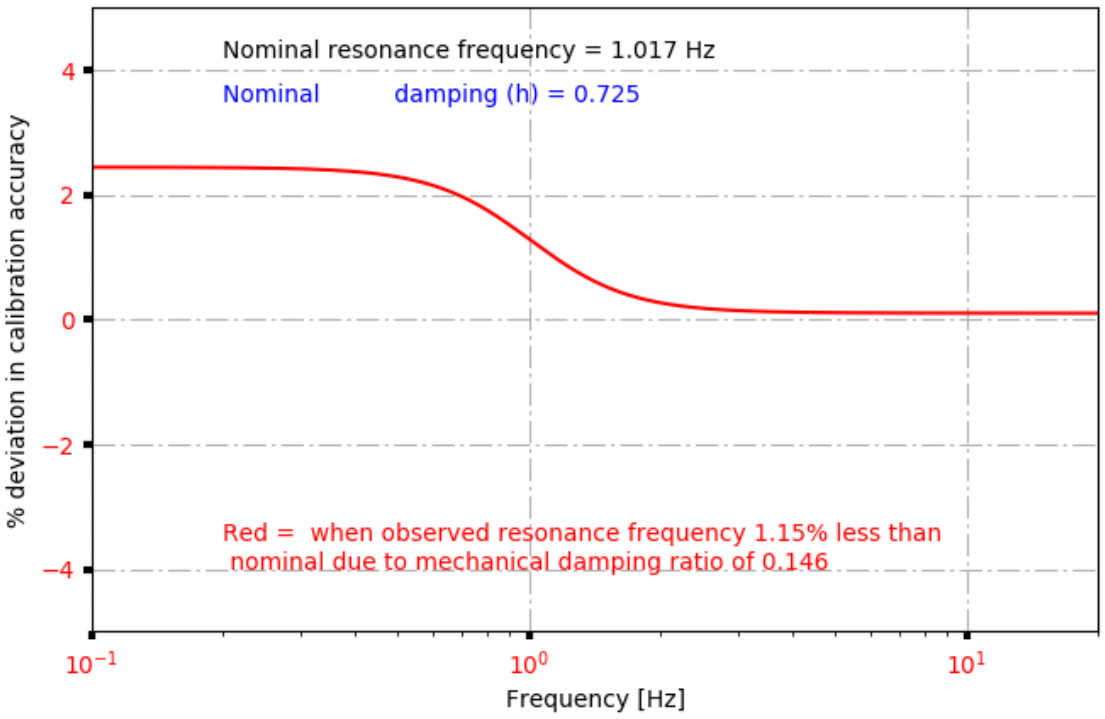

Figure 30: Frequency vs. %Deviation of accuracy in calibration when the resonance frequency deviates by -1.15 % due to mechanical damping radio of 0.146

6.1.8.5 Deviation in Free Period due to Quantization of FFT bins

Free Period is measured using a FFT in the frequency domain by finding the frequency with the highest energy spectra. A 4096 sample size is analyzed, that yields 2048 bins between dc and the Nyquist sampling frequency. The result is that the free period measurement falls within +/-1 bin of the peak. When testing 235 separate frequency measurements, varying from 0.1 Hz through 10 Hz, the maximum deviation (measured maximum – minimum) in frequency always fell within 1.4 % of the measured signal. A variance this small has negligible effect on the overall calculation of the instrument response. Therefore, quantization concerns can likely be ignored when estimating calibration uncertainty.

6.2 An Empirical Study of Calibration Accuracy using Multiple Calibrations

The discussion of section 6.1 concentrated on the variables that could influence the calibration and attempted to estimate the influence of each one on the overall response as a function of measurement error versus frequency. The largest influence appears to be the damping ratio: There is an almost 1:1 correlation on the response accuracy with the accurate measurement of damping ratio. The greatest effect occurs at the resonance frequency (Figure 29). Other variables, such as the accurate measurement of resonance frequency are also of importance, but these can be measured to great accuracy. Some variables, such as the gain of the digitizer channels will affect the measurement of the instrument sensitivity, but not the shape of the response. There are, however, other influences that are not as easily quantified. These influences we may term to be the "random" states that could include such things as the altitude, temperature, barometric pressure. It could include the self-noise of the seismometer, or changes in damping ratio due to dust, corrosion, or debris within the seismometer. It could include "dirty" sine-sweep time history data featuring teleseisms, office noise, or spurious impulses that inject energy into the sensitivity calculation. It could include small changes in measurement procedure that are related to the test operator. It could include non-linearities of the laser position sensor sensitivity with respect to offset, target irregularities, or temperature. For various reasons, all measurements have a degree of randomness that vary from test to test. This section attempts to quantify the effect of these random variables.

The randomness of the method was tested in two ways:

1) Ten separate calibrations of the same instrument over the course of several days.
2) A single continuous calibration with "dwell" time at each frequency in order to quantify how the sensitivity at each frequency varies with time.

Each test has its merits: The first test involved the set-up and tear-down of the entire calibration system: The laser was removed from the fixture, the seismometer was disconnected, mass locked,

repositioned, and then reconnected to the electronics. The seismometer mass was re-leveled. The damping ratio and resonance frequency were re-measured. The time of day was different. Thus, test method one is a measure of the day-to-day variances that likely involve not only the calibration variables, but also the environmental influences.

The second test looks at the randomness of the method and measurement instrumentation itself: Each excitation frequency used in the calibration was held constant for multiple minutes, and then a separate sensitivity calculation was made at that frequency by breaking the dwell time into discrete pieces of sixty seconds apiece. The sample size for each frequency measurement is fifteen samples, each of which is of sixty seconds-duration. The mean sensitivity for each frequency was then calculated, as was the range of the sample set, and the 2x standard deviation calculated in order to determine a measure of the randomness of the calibration. This test helps determine measurement consistency is when factors such as test setup, changes in weather, changes in technician technique, etc. are eliminated.

6.2.1 Calibration Scatter over Ten Separate Calibrations of the Same Instrument

Ten consecutive calibrations of an SM-3 seismometer were conducted to empirically estimate how consistent the calibration process is when repeatedly tearing down and setting up the system. Two different SM-3s were tested: SN337 and SN201. SN337 demonstrated some unexpected behavior between tests. It would “flip” it’s resonance frequency between two different values, likely because of an unstable balance spring within the unit. The SM-3 balance spring can easily rotate on its mount and may move to a different position when the seismometer is unlocked. SN337 was tested twice, and both times, the same behavior was observed. The resonance frequency of unit SN201 proved to be more stable, but also showed an occasional deviation in resonance frequency comparable to what is observed in SN337.

The calibration of the SM-3 seismometer consisted of using a sine sweep with a pre-established list of eighteen frequencies, ranging from 0.05 Hz through 10 Hz. The dwell time for each frequency was held to 60 seconds, and amplitude voltage was constrained to two different voltages: At 2.0 Hz and below, the excitation voltage was held to 2.0 V. At frequencies above 2.0 Hz, excitation voltage as set to 4.0 V. The calibrations were performed over the course of three hours to minimize any environmental changes that could influence the instrument response. The seismometer mass was locked after each test, the instrument was rotated 90 degrees, then the mass was unlocked and re-centered. This insured that each of the ten calibration tests were identical to one another, but also accounts for regular-world effects such as the setup and re-positioning of a seismometer in a vault or on a calibration pier.

The reported sensitivity of the seismometer is measured at 5 Hz, even though the curve continues to 10 Hz. At frequencies greater than 5 Hz, there is a large scatter in seismometer sensitivity, but this is attributable to a limitation in the measurement technology of the laser position sensor, and the signal coil's ability to generate sufficient mass motion at higher frequencies. (discussed in section 6.3).

6.2.1.1 SM-3 SN201: Calibration Scatter over 10 Separate Calibrations

SM-3 SN201 is a 40 year-old Soviet Electro-mechanical seismometer that is configured for use with an analog seismic station. It demonstrates good performance in terms of sensitivity (Figure 31). The calibration matrix shows good consistency for all measured parameters: Resonance frequency excepted, the first calibration reported a resonance frequency of 1.11 Hz, which represents about a three percent deviation from the mean of 1.083 Hz (Table 8). Analysis of the raw time-history data demonstrates that this was not a FFT binning issue, but represents a real shift in the resonance frequency. The same phenomenon is observed in the other SM-3 used in this test. However, all subsequent calibrations were identically measured at 1.081 Hz. During the ten calibrations, damping ratio demonstrated a standard deviation of 1.2 percent. Sensitivity at 5Hz varied with a standard deviation of 2.42 percent; It is therefore a reasonable estimate that accuracy in calibration due to set-up, tear-down for this instrument should fall within two standard deviations, or 4.84 percent. The estimate of 1.2 % for deviation in damping ratio appears to be in-line with the estimates discussed in section 6.1.8.2

Calibration Statistics from SM-3 SN201 for 10 calibrations				
CAL#	Damping (h)	Resonance (Hz)	Sensitivity @ 5Hz (V.sec/m)	%deviation from mean
1	0.582	1.11	74.123	1.9%
2	0.576	1.08	75.611	4.0%
3	0.584	1.08	74.904	3.0%
4	0.572	1.08	70.969	-2.4%
5	0.591	1.08	73.431	1.0%
6	0.588	1.08	70.243	-3.4%
7	0.593	1.08	72.732	0.0%
8	0.587	1.08	73.021	0.4%
9	0.595	1.08	71.700	-1.4%
10	0.586	1.08	70.476	-3.1%
Mean	0.585	1.083	72.721	
Std. Dev	0.007	0.009	1.760	
Percentage Stdev/Mean	1.17%	0.83%	2.42%	

Table 8: SN201 Calibration Matrix Results. Sensitivity is reported at 5 Hz. The standard deviation of sensitivity is 1.76 V.sec/m, representing 2.42 % of the measured signal.

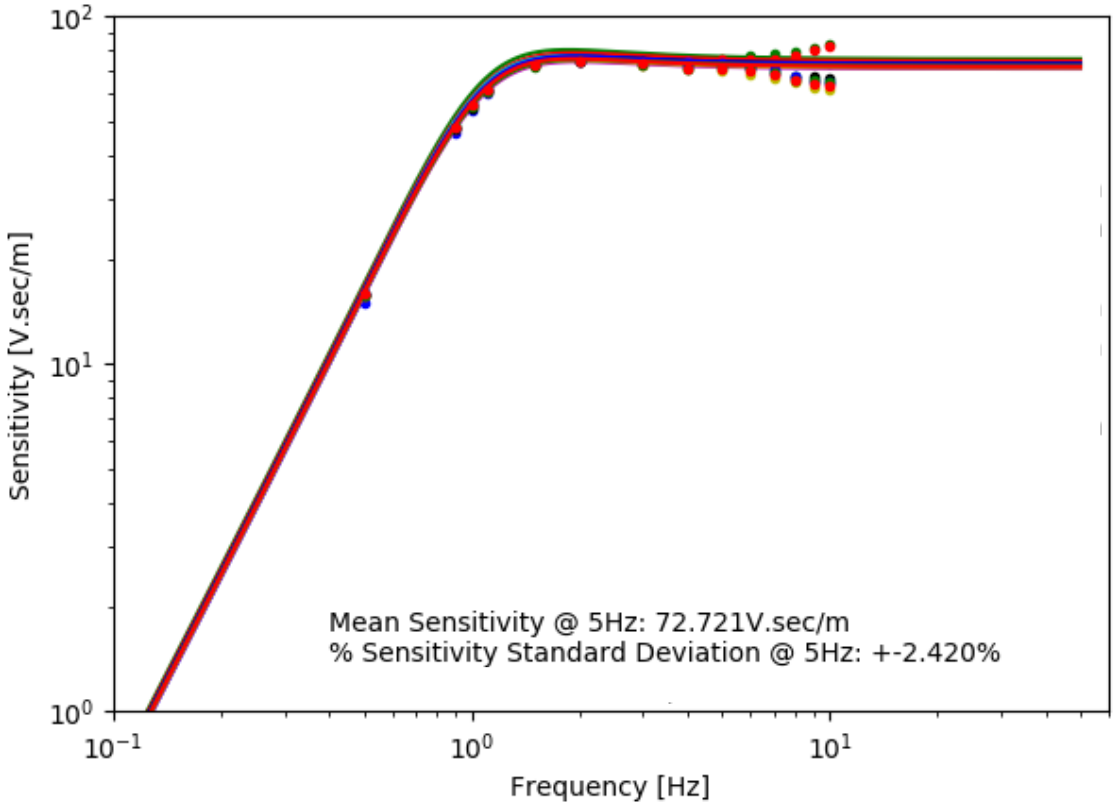

Figure 31: Calibration curves for SM-3 SN201. Solid lines represent Poles & Zeros estimation of response whereas dots represent sensitivity points at frequency. Frequencies greater than 5 Hz scatter because of LK-G32 laser position sensor limitation and insufficient mass motion.

6.2.1.2 SM-3 SN337: Calibration Scatter over 12 Separate Calibrations

SM-3 SN337 calibration study is similar to the previously mentioned seismometer (SN201) except it exhibits a troubling mechanical issue: When unlocking and re-locking the mass, the seismometer will ‘pop’ back and forth between two different resonance frequencies (Figure 32). The best hypothesis is that the balance spring clicks back and forth between two positions. The raw data confirms that this is a real change in resonance, and not an effect of the calibration process itself (Table 9). Therefore, the three percent deviation in resonance frequency should be discounted in terms of measurement uncertainty, because it is a real change to the response. The seismometer does however, demonstrate that damping ratio deviates at the same percentage of 1.2 % as that of SN201. It also shows a 1.53 % standard deviation in sensitivity at 5Hz, which is likely less than that of SN201 because this seismometer is more sensitive and has a better signal to noise ratio. Therefore, the assumption of 2X Standard Deviation of 4.84 % as the upper bound for calibration uncertainty in terms of sensitivity is still likely a good estimate, even with seismometers that exhibit some variation in resonance frequency.

Calibration Statistics from SM-3 SN337 for 12 calibrations				
CAL#	Damping (h)	Resonance (Hz)	Sensitivity @ 5Hz (V.sec/m)	%deviation from mean
1	0.558	0.89	186.251	-2.5%
2	0.583	0.89	192.874	1.0%
3	0.567	0.954	187.908	-1.6%
4	0.578	0.89	185.035	-3.1%
5	0.568	0.954	194.491	1.8%
6	0.580	0.89	192.329	0.7%
7	0.572	0.954	193.028	1.0%
8	0.573	0.954	191.959	0.5%
9	0.579	0.89	192.012	0.5%
10	0.574	0.89	192.035	0.5%
11	0.583	0.89	194.105	1.6%
12	0.574	0.954	190.414	-0.3%
Mean	0.574	0.917	191.037	
Std. Dev	0.007	0.031	3.031	
percentage Stdev/Mean	1.23%	3.42%	1.59%	

Table 9 Calibration statistics for SM-3 SN337. This seismometer features a real deviation in resonance frequency and is not related to the calibration method. Sensitivity standard deviation varies at 5 Hz by 2.9 V.sec/m (1.53 percent of measured signal)

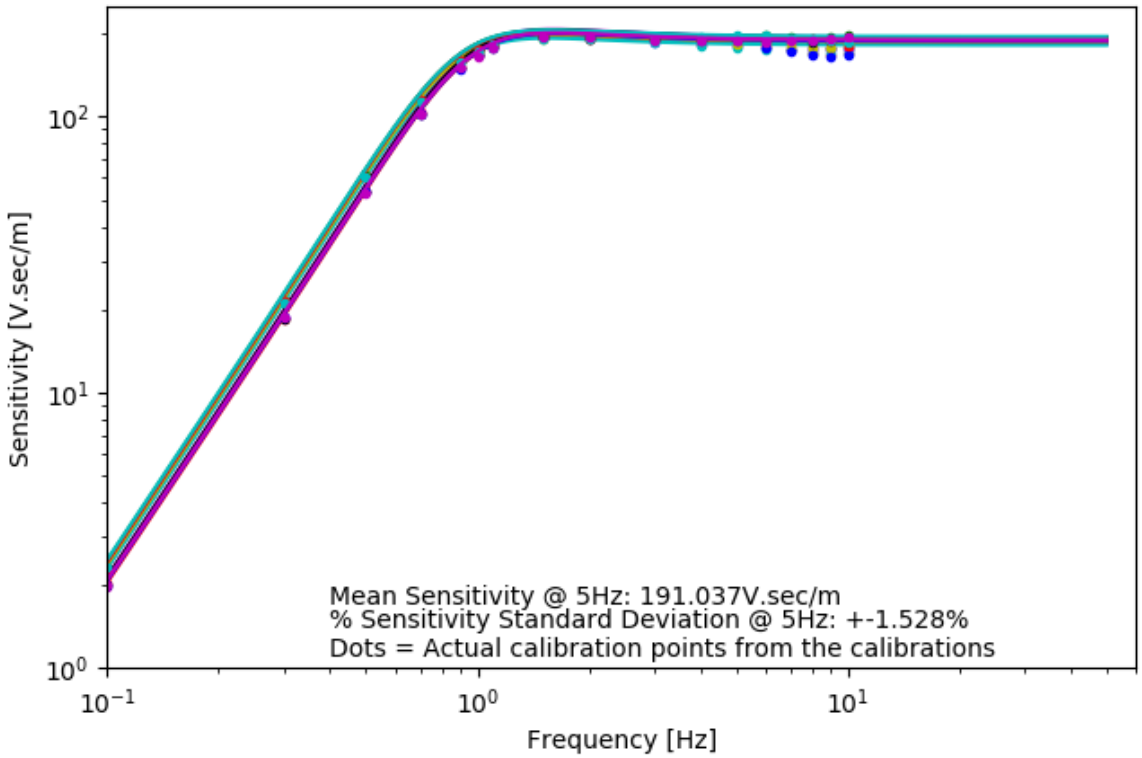

Figure 32: Calibration curves for SM-3 SN337. Solid lines represent Poles & Zeros estimation of response whereas dots represent measured sensitivity points at frequency.

6.2.2 Calibration Sensitivity Scatter over a 4-hour Test

The Calibration sensitivity scatter test lends insight into the stability of seismometer signal (in unknown units of velocity) to seismometer mass displacement (in known units of displacement). In this case, the system is calibrated once, but is forced to dwell at each frequency so that multiple measurement points are recorded and calculated. The result is that one can then apply a measure of statistics to each frequency and judge the uncertainty of the measurement algorithm as a function of frequency. Like the tests of damping ratio and oscillation frequency (section 6.1.8), this test yields insight into the stability of the test during calculation of both velocity signal voltage and ground displacement. The deviation as a percentage is measured as a function of frequency. Any deviation in the test will be due to stability variations in the measurement of the seismometer signal coil, or in the measurement of the seismometer mass displacement. Because the test involves a pure sine-based signal, velocity and displacement are mathematically related to one another by a simple phase shift. The calibration method was tested by collecting 270 separate frequency points over the span of four hours. The signal generator dwelled at a discrete frequency for fifteen minutes at a time, and the time-history record was split into one-minute files. This enabled the calibration algorithm to create multiple sensitivity calculations at each frequency (Figure 33). Any deviation in amplitude at each frequency should be a result of a convolution of seismometer mechanical and electrical noise, ground motion measurement uncertainty, and signal coil voltage measurement uncertainty. The two remaining uncertainties; damping ratio and free period, are held as constants for this test. The seismometer used for this test is the MSU Soviet-made SM-3 serial number 201.

As the dwell test progresses from low frequency to higher frequencies, the range of calculated sensitivities at each frequency remains below one percent, (Except for 0.1 Hz, which lies outside the bandwidth of the seismometer. It was tested just to be consistent with prior testing) until the frequency exceeds 5 Hz. At this point, the measurements begin to diverge from point to point (Table

10). This is likely why Figure 33 shows a strange ‘tail’ above 5 Hz: This is due to insufficient mass motion of less than 50 microns, which enables the 0.5 micron uncertainty of the laser to adversely affect the instrument sensitivity accuracy (See sec. 6.1.4.1). When one plots the percentage variation of sensitivity as a function of frequency, it demonstrates that the 2X Standard deviation does not exceed 1 % until greater than 5 Hz (Figure 34). Therefore, it is advised that until the issue of insufficient ground motion at higher frequencies is addressed, the calibration be limited to 5 Hz. This is sufficient to elicit an acceptable two poles and zeroes solution.

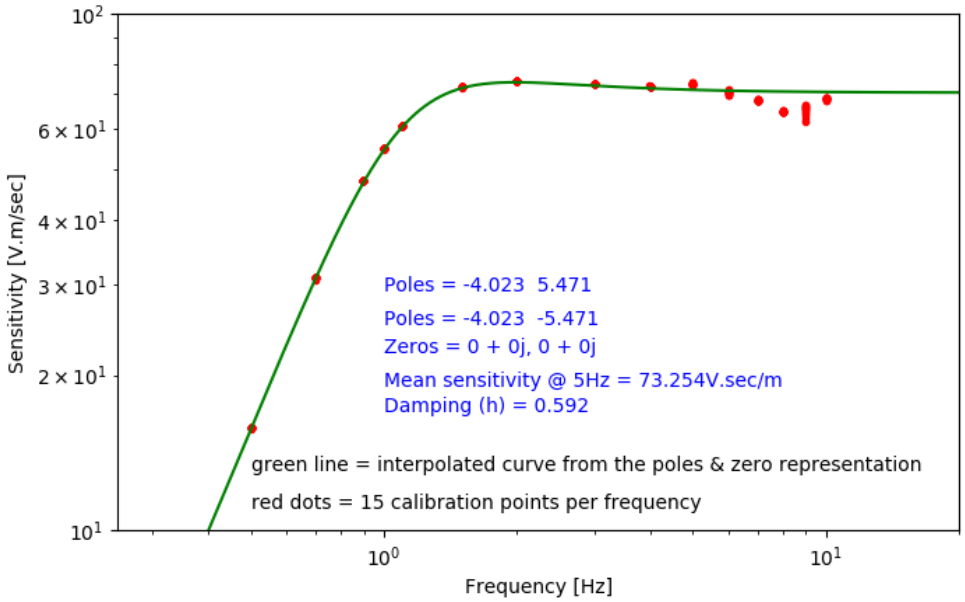

Figure 33: Calibration curve of SM-3 SN201, showing scatter of 15 measurement points per frequency, between 0.1 Hz and 10 Hz. Computed sensitivity varies by less than one percent until frequency exceeds 5 Hz, where hardware limitations of the laser measurement system cause drift of the sensitivity calculation.

# measurement points	Frequency (Hz)	Sensitivity Mean (V.sec/m)	Sensitivity StDev	Sensitivity Range	% StDev/Mean	%Deviation of Range
14	0.1	0.62	0.003	0.01	0.50	2.1
15	0.3	5.57	0.009	0.04	0.20	0.6
15	0.5	15.79	0.003	0.01	0.00	0.1
15	0.7	30.85	0.077	0.31	0.30	1.0
16	0.9	47.50	0.004	0.02	0.00	0.0
15	1.0	54.84	0.061	0.25	0.10	0.4
15	1.1	60.82	0.012	0.05	0.00	0.1
15	1.5	72.29	0.076	0.32	0.10	0.4
15	2.0	74.11	0.020	0.07	0.00	0.1
15	3.0	73.36	0.058	0.18	0.10	0.3
15	4.0	72.42	0.104	0.47	0.10	0.6
15	5.0	73.25	0.211	0.71	0.30	1.0
15	6.0	70.57	0.560	2.07	0.80	2.9
15	7.0	68.20	0.163	0.59	0.20	0.9
15	8.0	64.80	0.090	0.24	0.10	0.4
15	9.0	64.98	1.502	4.64	2.30	7.1
15	10.0	68.53	0.261	0.90	0.40	1.3

Table 10: Sensitivity scatter as a function of frequency for SM-3 SN201. Note that the % deviation of sensitivity range and standard deviation remain below one percent until frequency rises above 5 Hz. This is due to hardware limitations in the laser measurement system and excitation coil ability to generate sufficient ground motion.

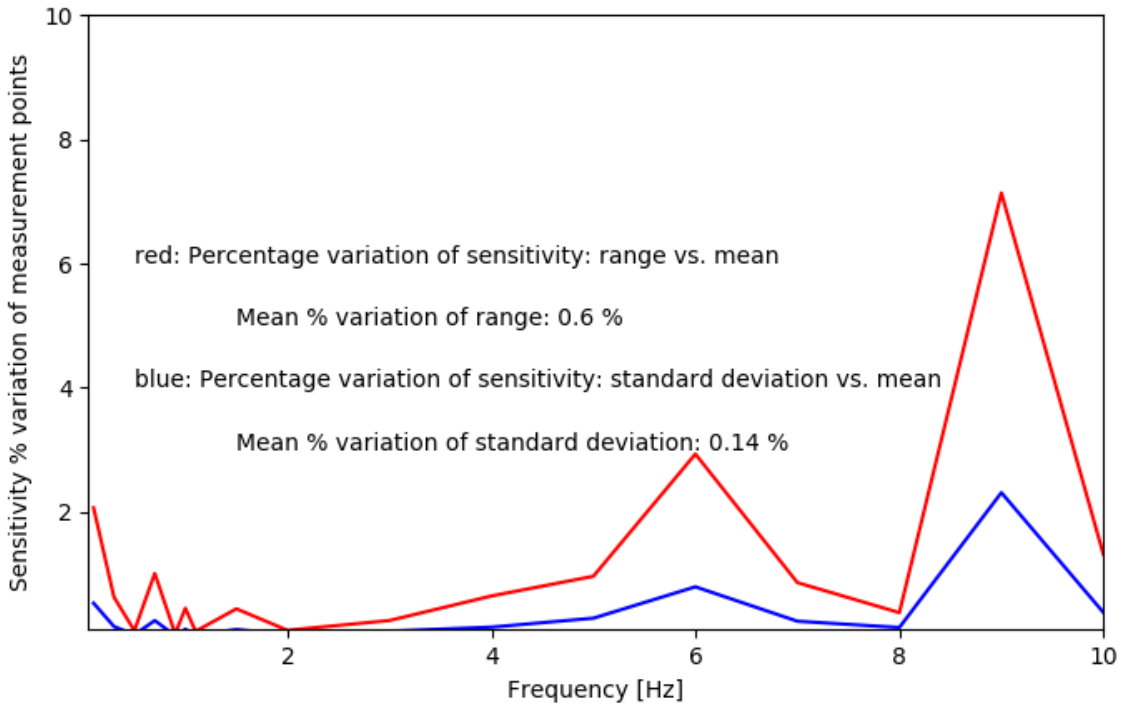

Figure 34: Sensitivity Scatter as a function of frequency, 15 measurement points per frequency. Red line represents the observed max-min (range) of each frequency as expressed in percentage of its respective amplitude. Blue line represents two standard deviations of sensitivity as a percentage of its respective amplitude. (semi-log plot of frequency). Note that uncertainty rises beginning at 5 Hz. This is due to insufficient mass displacement and hardware limitations of the laser.

6.3 Mass Displacement Tracking Calibration: Best Estimate of Accuracy

The previous sections 6.1 through 6.2 provide an estimate of calibration accuracy as a function of frequency. Section 6.1 covers the variables within the calibration that influence accuracy. Of all the variables that can influence accuracy, it is the measurement of damping ratio that appears to cause the most deviation in calibration (Section 6.1.8.1). Based on this section, it is expected that with a 0.52 % standard deviation in damping ratio, the absolute best one should expect for peak uncertainty in terms of sensitivity (Figure 29), should be about 1.05 %. Section 6.2 provides an empirical measurement of a more realistic measure of calibration uncertainty. In the real world, multiple calibrations of the SM-3 seismometer in section 6.2.1 provides an empirical estimate of calibration accuracy. Two separate seismometers of the same model were tested. By estimating peak sensitivity at 5 Hz, both standard deviations (2.48 % and 1.52 %) should be close to realistic estimates (Figure 31 and Figure 32). One can estimate the uncertainty of the calibration by multiplying the highest standard deviation by two. Thus, in practice, the MDT calibration method should result in a best estimate of sensitivity at +/- 4.96 percent or better.

6.4 Co-location of Calibrated Seismometer with Reference Seismometer

The final proof of 'how accurate' this method can be is a co-location demonstration based on a reference broad-band instrument with an Electro-mechanical seismometer that has been calibrated using the MDT calibration method. The reference seismometer is a Guralp CMG-3T that was last calibrated during manufacturing, in 1987. This instrument was serviced by Guralp in 2016, and thus the calibration should be within manufacturers specification. Communication with the manufacturer confirms that the Guralp CMG-3T generally does not drift away from its initial calibration over its service lifetime, and that the initial calibration should still be valid.

A Geotech S-13 vertical instrument was calibrated using the MDT calibration method and was then co-located with the Guralp CMG-3T. A sixty-minute test of the two instruments was then analyzed

using a Power Spectral Density (PSD) analysis to show energy from ambient seismic noise (Figure 35). Because the Geotech S-13 is a short-period instrument, the PSD analysis is restricted between 0.125 Hz and 15 Hz, which falls within the published passband of the short-period instrument. If the calibration of the Geotech, based on the MDT calibration method is accurate, the ambient noise as expressed by both instruments in the frequency domain should fall within the same line. Any differences are either a function of the calibration deviation of the Geotech S-13 or from the original CMG-3T calibration.

After calibration, the largest deviation when comparing noise of the two instruments occurs at 1.5 Hz, with a maximum deviation of +1.5 dB. The remaining portions of the curve, from 0.125 Hz to 15 Hz track within a fraction of a decibel of the reference seismometer (Figure 35). Based on these results, it would be fair to conclude that the MDT calibration method can provide a viable calibration alternative to other less portable, and more expensive methods.

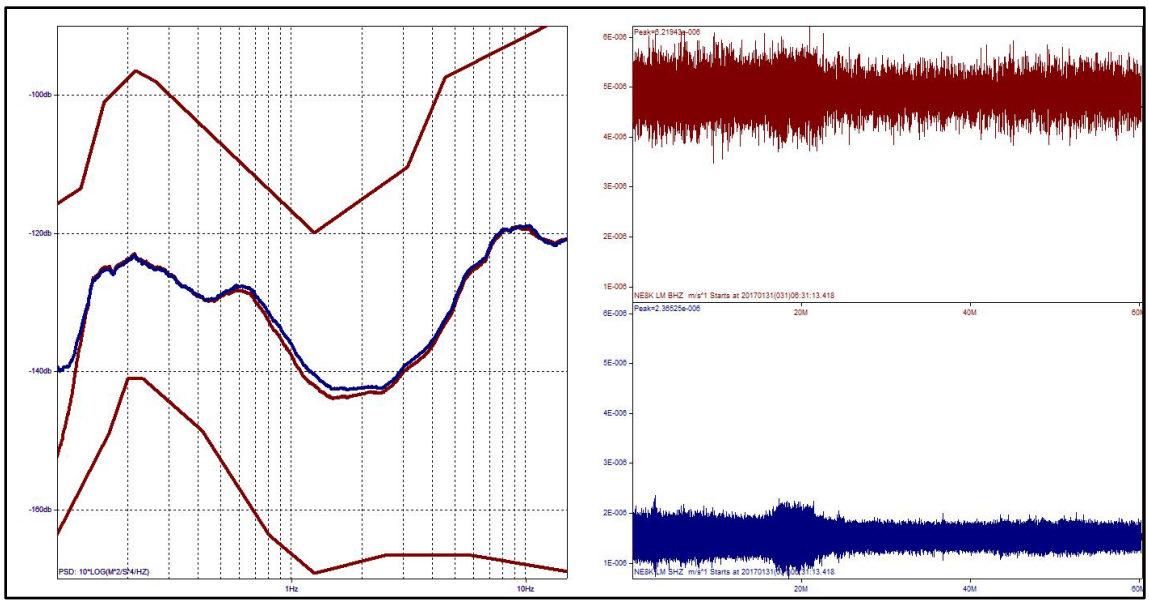

Figure 35: Co-location of a Guralp CMG-3T (red waveform) with a Geotech S-13 (blue wafeform) that was calibrated with the MDT calibration method. A 60-minute ambient noise PSD comparison shows both seismometers in agreement at all frequencies between 0.15 to 15Hz, to less than 1.5 decibel. Frequency domain is shown on the left, Time domain of the same data is shown on the right. The upper red line represents the New High Noise Model(NHNM) whereas the lower line represents the New Low Noise Model (NLNM). Nearly all seismic station noise profiles throughout the world fall within these two lines.

CHAPTER 7: CONCLUSION

We have developed a straightforward "cookbook" procedure for calibration of the Electro-mechanical seismometer, which is still commonly found in seismic networks throughout the world. By using the optical displacement transducer, we avoid a significant amount of math and measurement error commonly associated with the use of force calculations necessary with the calibration coil method. This end-to-end calibration optically measures mass movement to determine actual ground motion and corresponding ground velocity. The procedure then compares ground velocity to the recorded voltage output generated by the seismometer. By measuring the corresponding voltage output at multiple frequencies across the passband, we re-create the frequency response curve of the instrument. This general-purpose method applies to any seismometer where the mass can be exposed for optical tracking, and it can be deployed in the field for the quick calculation of instrument response.

7.1 Current Limitations to the calibration method

The method works for short period Electro-mechanical instruments and holds accuracy to within five percent up to 5 Hz. At higher frequencies, laser measurement system and mass displacement limitations result in less and less accurate measurements as a function of frequency. By the time the sine sweep excitation of the instrument reaches 10 Hz, accuracy degrades to ten percent because of insufficient mass motion, dc drift, and frequency-dependent non-linearity of the laser. Therefore, this method is good only for when one requires only a two poles, two zeros solution to the instrument response, to describe instrument response to 5 Hz, and it assumes that response is then flat for all higher frequencies. Most seismometers exhibit a flat response beyond this frequency until roll-off occurs at some unspecified high frequency, likely beyond 20 Hz. We are unable to observe the roll-off using this method, because observation of instrument roll-off at higher frequencies is beyond the technical limitations of the laser.

7.2 Seismometers Adapted to Use the Laser Position Sensor

To date, we have successfully applied the calibration method to the Soviet/Russian SM-3 vertical and horizontal (Figure 21), SKM vertical(Figure 36), SKM Horizontal, SKD vertical, S1-P (Figure 37), and VEGIK(Figure 38) seismometer. These seismometer models comprise the vast majority of all Electro-mechanical instruments still in permanent use throughout states of the Former Soviet Union. Additionally, we have successfully calibrated several dozen Geotech S-13 seismometers from the IRIS/PASSCAL instrument pool. (Figure 39) (Burk *et al*., 2015)

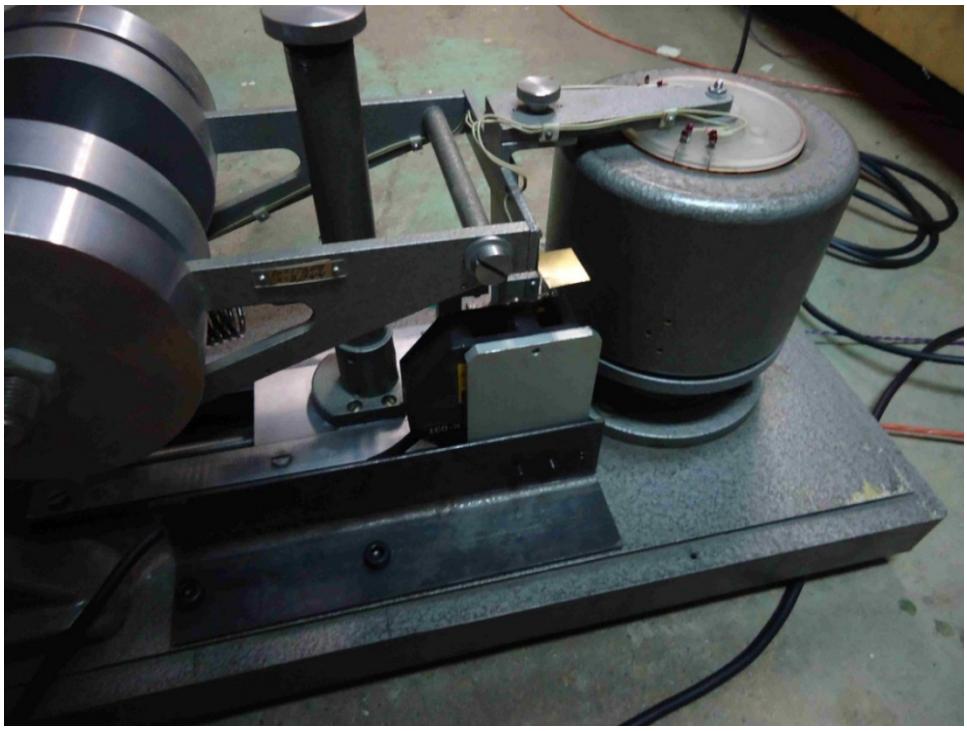

Figure 36: The LK-31 laser mounted on an SKM-V seismometer. The laser measures displacement via the brass reflector that is permanently attached to the pendulum arm.

Figure 37: S1-P Seismometer, as used in Kazakhstan, with custom laser mounting bracket.

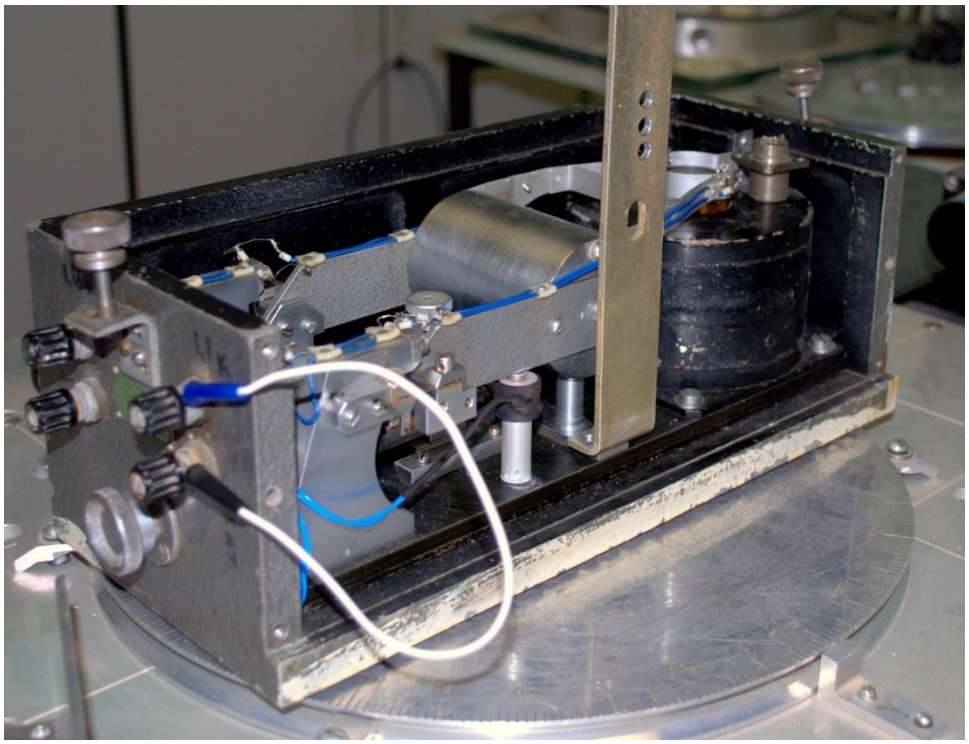

Figure 38: VEGIK seismometer, circa 1965. These seismometers are retained in some networks in eastern Europe.

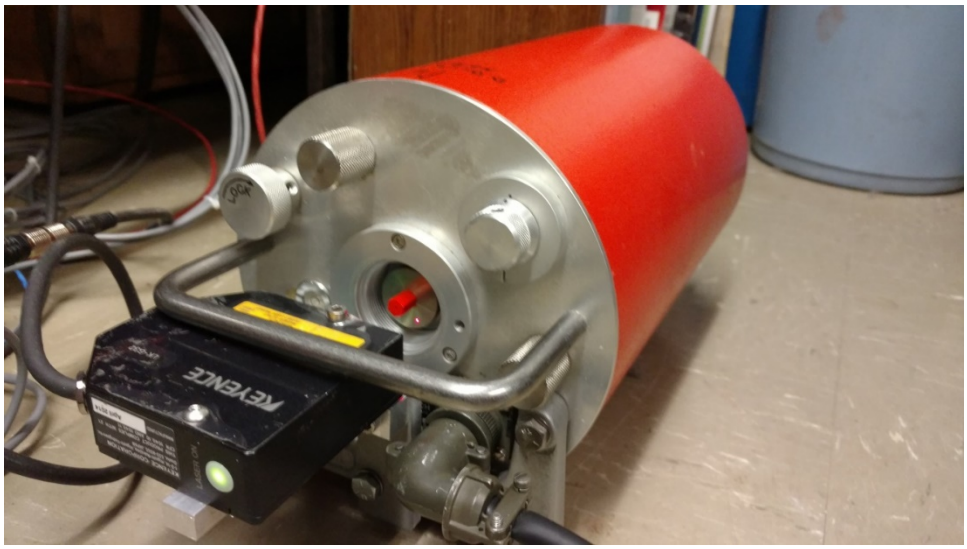

Figure 39: Calibration fixture for the Geotech S-13 seismometer

7.3 Future Use of the Calibration Method

It is possible to quickly check calibration on seismometer models in order to test for repeatability. This may be beneficial for places where it is difficult or impractical to calibrate all seismometers and configurations. Such might be the case with station configurations that may no longer exist, but the data remains within archives. We have begun to calibrate increasing numbers of instruments in order to estimate the 'spread' of instrument sensitivity as well as the change in gain over time. By calibrating a statistically significant number of instruments, it may be possible to establish a 'base line' calibration for a given instrument model, as well as provide an uncertainty. This creation of a more accurate estimate of response would then improve the metadata for the archived data that is found throughout the world's local and regional networks.

BIBLIOGRAPHY

BIBLIOGRAPHY

Beyreuther, M., R. Barsch, L. Krischer, T. Megies, Y. Behr, and J. Wassermann (2010). ObSpy: a Python Toolbox for Seismology, *Seismological Research Letters* **81**, 530-533.

Burk, D., Mackey, K., and Hartse, H. (2015). A Field Calibration Method for Digitized Electro-Mechanical Seismometers, Abstract T3.1-P2, *CTBT: Science and Technology Conference 2015 Book of Abstracts*, Vienna, Austria, p. 112.

Halliday, D., R. Resnick, and L. Walker (2011). *Fundamentals of Physics* (9th ed.), John Wiley & Sons, Hoboken, NJ, USA, 1248 pp.

Havskov, J., and G. Alguacil (2004). *Instrumentation in Earthquake Seismology,* Springer, Dordrecht, Netherlands, 360 pp.

Malovichko, A.A. (editor), (2015). *Earthquakes of Russia in 2013,* Geophysical Survey, Russian Academy of Sciences, Obninsk, Russia, 224 pp. (in Russian)

Rodgers, P.W. (1995). Signal-Coil Calibration of Electromagnetic Seismometers, *Bulletin of the Seismological Society of America* **85**, 845-850.

Scherbaum, F. (2001). *Of Poles and Zeros* (2nd ed.), Kluwer Academic Publishers, Dordrecht, Netherlands, 256 pp.

Stein, S., and M. Wysession (2003). *An Introduction to Seismology, Earthquakes, and Earth Structure.* Blackwell Publishing, Malden, MA, 498 pp.

Wenner, F. (1929). A New seismometer equipped for electromagnetic damping and electromagnetic and optical magnification, *Bureau of Standards Journal of Research* **2,** 963-999.